EFFECTS OF VARIATION OF THE MODIFYING CTBN ELASTOMER IN THERMOSET POLYMERS

by

Harold Pierce Martin

EFFECTS OF VARIATION OF THE MODIFYING CTBN ELASTOMER IN THERMOSET POLYMERS

BY

HAROLD PIERCE MARTIN
B.S., United States Naval Academy
(1961)

Submitted in partial fulfillment
of the requirements for the degrees of

Naval Engineer and Master of Science
in Naval Architecture and Marine Engineering

at the

Massachusetts Institute of Technology
(June 1971)

ABSTRACT

EFFECTS OF VARIATION OF THE MODIFYING CTBN ELASTOMER IN THERMOSET POLYMERS

by

HAROLD PIERCE MARTIN

Submitted to the Department of Naval Architecture and Marine Engineering on May 14, 1971, in partial fulfillment of the requirements for the degree of Naval Engineer and Master of Science in Naval Architecture and Marine Engineering.

A method of optimizing the toughness of elastomer modified epoxy resins without significantly sacrificing material strength was investigated utilizing flat plate castings machined into cleavage and tensile specimens. The method selected was to toughen the epoxy matrix by inclusion of various CTBN elastomer particles in combinations not to exceed 10 pph. The Hycar CTBN liquid polymers were prepared especially to show the importance of molecular weight, acrylonitrile content, and particle size in optimizing for tougher thermosetting polymers. It was found that by combining two different elastomers in a constant CTBN elastomer concentration of 10% by weight, the optimum toughening of the epoxy matrix can be achieved and yet not sacrifice appreciable strength and ductility of the material. It was further hypothesized that the optimum toughening of the matrix was achieved through the flexibility of the molecular network.

The yield behavior of a glassy polymer was investigated under a system of biaxial stress in an attempt to define a criterion for yield. By subjecting unmodified and elastomer modified epoxy, EPON 828, biaxial compressive cylinders to a biaxial stress field, it was possible to obtain yield envelopes which were indicative of the modes of failure taking place. It was found that biaxial specimens of EPON 828 (unmodified) and with CTBN 20-64 (small elastomer particles) yielded in a ductile manner exhibiting the shear yielding criterion of Mohr-Coulomb with no macroscopic evidence of stress whitening, crazing or void formation. Biaxial specimens of CTBN 151W, consisting of large elastomer particles, suggested two distinct yield criterions with a Tresca maximum shear criterion appearing most valid in the first quadrant and a Mohr-Coulomb criterion in the second quadrant. It appears that future work should direct its analysis to both quadrants simultaneously in order to arrive at a general yield criterion.

ACKNOWLEDGMENTS

The author wishes to express his gratitude to Professor F. J. McGarry, his thesis advisor, for the opportunity to do this work and especially for his valuable advice and suggestions during the preparation of this thesis. The author would also like to express his appreciation to Professor J. N. Sultan for his supervision and invaluable comments.

The author sincerely appreciated the cooperation from the Civil Engineering Department's Materials Division personnel. The author is especially indebted to Arthur Rudolph, James King and John Mandell for their assistance.

Finally, I wish to dedicate this work to my wife, Jane, without whose encouragement, understanding and patience this thesis would never have been possible.

TABLE OF CONTENTS

TABLE OF CONTENTS (CONTINUED)

CHAPTER I

Introduction

Epoxy resins are classified as glassy thermosetting plastics. These resins make an excellent matrix material because of their versatility, good handling characteristics, low shrinkage, excellent adhesive properties and good mechanical properties; however, in an unmodified state, they are inherently brittle and susceptible to catastrophic failure. This study was conducted to achieve the greatest usefulness of the CTBN elastomer in toughening the epoxy matrix with minimal sacrifice of desirable properties. In addition, a biaxial stress study investigates the yield criterion (s) associated with the epoxy matrix modified with CTBN elastomer.

Elastomer particles in glassy polymer matrix materials can increase fracture surface energy by as much as an order of magnitude over that of unmodified material (1) and product stress whitening (2) and shear bands (3) in tensile specimens.

McGarry and Stegeman (4) attempted to increase the fracture toughness of epoxy and polyester resins by introduction of a fine dispersion of polyethylene particles into the glassy matrix. It was discovered that the polyethylene was detrimental rather than beneficial in terms of improving the toughness of the resins, probably because of poor inter-

facial bonding. By introduction of elastomeric particles into the glassy polymer matrix material, Buchnall and Smith (2) found that a finely dispersed secondary phase of these particles became chemically bonded to the matrix material. These particles will cause the polymer to flow locally in the regions of high stress. A further result of this investigation showed that small concentrations of these elastomers were highly effective in increasing the energy to produce fracture by greatly increasing the volume of matrix material which crazes or cold draws prior to fracture.

In a latter investigation, Sultan and McGarry (5) found that by introducing into the polyester prepolymer a low concentration of an elastomer having reactive sites such as carboxyl-terminated butadiene-acrylonitrile copolymer (Hycar CTBN), it is possible to capitalize on this ability of the polyester to cold flow locally and thereby increase the fracture toughness by a factor of 8-11. Attempts to so modify other similar polyester resins with other elastomers such as butadiene-styrene copolymer were not as successful.

The efficiency of reinforcement by the elastomer depend upon a number of factors, not all of which are entirely clear. Included among these are the nature of the elastomer, its particle size, the particle size distribution, the difference in elastic constants of the rubbery and glassy

phases, the continuity of porosity of the individual rubber particles and the adhesion between particles and matrix as related to potential reactions between the two (6).

The optimum system for toughening of a brittle epoxy matrix was proposed (7) to be one in which an elastomer having primary reactive sites can be dissolved in the epoxy prepolymer and caused to precipitate out as a second phase during the gelling and cross linking reaction of the epoxy. The reactive sites would be available for formation of primary bonds between regions of high elastomer concentration and a matrix composed principally of epoxy. Experimental investigation (8) utilizing such a system showed that fracture energy of elastomer modified EPON 828 epoxy* material polymerized with Curing Agent D* was found to increase with increasing size and concentration of precipitated CTBN** elastomer particles at a single elastomer concentration. Particle sizes, ranging from 200-12,000 angstroms, were fairly independent of curing temperature and elastomer molecular weight. Final particle sizes tended to be affected by variations of acrylonitrile content in the CTBN elastomer molecule.

Sternstein and Ongchin (9,10) investigated criteria for normal stress yielding (crazing) and shear yielding

---

*Manufactured by Shell Chemical Co., New York City, N. Y.

**Hycar Rubber, B. F. Goodrich Chemical Co., Cleveland, Ohio

using samples machined from cast solid cylinders of PMMA. Combinations of biaxial stress ranging from uniaxial tension to equal biaxial tension were used in both the crazing and shear yielding studies. For the shear yielding study, the samples were internally pressurized and immediately subjected to a constant axial strain rate until the yield point was reached. For the crazing study, the tubes were pressurized, brought to a given level of axial load, and held in this state of biaxial stress for ten minutes at which time crazing began to appear. Each yielding mode produced curves of distinctly different form with symmetry about the equal biaxial stress line. The experimental data yielded a series of craze yielding envelppes as functions of stress and temperature. Shear yielding was shown to be consistent with the three dimensional analog of the Mohr-Coulomb criterion. The results of this investigation showed that two forms of yielding in glassy PMMA may be characterized with respect to their stress field dependencies.

The yield behavior of an amorphous glassy polymer has been investigated (11) under a system of combined stress in an attempt to define a criterion for yield. Sheets of polymethylmethacrylate were compressed in plane strain, and the compressive yield stress was determined as a function of the tension applied in the plane of the sheet. The compressive yield stress was found to decrease with applied tension more rapidly than would be expected if the

shear yield stress of the material were independent of pressure. The results were analyzed in terms of a Coulomb yield criterion where the shear yield stress is expressed as a constant plus a friction term proportional to the pressure on the shear plane.

A recent investigation by Bowden and Jukes (12) conducted plane strain compression tests on a number of materials including PMMA. The shear yield stresses of all these materials were pressure-dependent. It was shown that for PMMA the yield stress in simple compression is significantly less than the plane-strain compressive yield stress, thus these results indicated that the shear stress cannot depend only on the pressure on the shear plane. Considering the large compressibility of polymers, an attractive hypothesis is that the yield stress is controlled by molecular chain segment mobility which is in turn directly related to the hydrostatic component of the applied stress system. This idea has been well expressed by Sternstein and Ongchin (9, 10) who propose essentially a von Mises criterion for yield. The results of this study verified the viewpoint of Sternstein and Ongchin with respect to the yield criterion of PMMA that a von Mises criterion is the one most appropriate.

CHAPTER II

Materials Investigated

All specimen castings used EPON 828 resin, an epichlorhydrin/bisphenol A product with an epoxide equivalent of 185-205 which was polymerized with 5% by weight of Curing Agent D, the tri (2-ethyl hexanoic acid) salt 2, 4, 6 tri (dimethyl aminomethyl) phenol.

The modifying elastomer (Hycar CTBN) was a random liquid copolymer of acrylonitrile and butadiene. It may be represented structurally, for most purposes as follows (13):

$$HOOC\text{-}[\text{-}(CH_2CH = CHCH_2)_X(CH_2\underset{\underset{C\equiv N}{|}}{CH})_Y]_Z\text{-}COOH$$

where averaged, X = 5, Y = 1, Z = 10. Hycar CTBN may be thought of as a dicarboxylic acid in regard to its reaction chemistry. It follows the crosslinking and chain-extension reactions for carboxylic elastomers.

The carboxyl groups at each end of the CTBN molecule are considered to be reactive sites possessing the ability for the liquid elastomer to polymerize and crosslink with other rubber molecules to form particles and also to provide the primary bonds between elastomeric molecules and the epoxy resin, forming an adhesive bond between the rubbery second phase and the glassy matrix (7). The Hycar CTBN liquid polymers will cure with epoxy resins over a wide

range of compositions.

All specimen types, modified by inclusion of an elastomer, contained 10% by weight of Hycar CTBN. All castings were cured at 120°C for two hours, slowly cooled to 50°C and then post cured at 130°C for two hours followed by slow cooling to room temperature.

Two different CTBN elastomer compositions were employed in modifying the thermoset epoxy materials used in specimen casting procedures of Appendices A and B, possessing the following parameters (13):

Elastomer/ Polymer Symbol	$\overline{Mn}$	% Acrylonitrile	% Butadiene	Solubility Parameter
EPON 828	360	--	--	9.16
CTBN R-151W	4700	18.2	81.8	8.77
CTBN 20-64	3000	28.0	72.0	9.14

CHAPTER III

Experimental Technique

A. Introduction

Experimental procedures for this study included:

1. Cleavage tests which determined the fracture surface work, γ, using an Instron Testing Machine.
2. Uniaxial tensile tests which determined the ultimate tensile strength using an Instron Testing Machine.
3. Biaxial stress tests conducted by the apparatus shown in figure (1) and being applied to hollow cylindrical specimens as shown in figures (5 and 6).
4. Uniaxial compressive tests which determine the ultimate compressive strength using an Instron Testing Machine.
5. Optical microscopy of cleavage and biaxial specimen surfaces using reflected light of a Reichert microscope.
6. Electron scanning microscopy of cleavage and tensile specimen fracture surfaces.
7. Electron transmission microscopy of smooth flat plate castings.

Experiments were conducted on seven material

compositions which included:

1. EPON 828 - 5% Curing Agent D
2. EPON 828 - 5% Curing Agent D - 10% CTBN 20-64
3. EPON 828 - 5% Curing Agent D - 10% CTBN 151W
4. EPON 828 - 5% Curing Agent D - 8% CTBN 151W 2% CTBN 20-64
5. EPON 828 - 5% Curing Agent D - 6% CTBN 151W - 4% CTBN 20-64
6. EPON 828 - 5% Curing Agent D - 4% CTBN 151W - 6% CTBN 20-64
7. EPON 828-5% Curing Agent D - 2% CTBN 151W - 8% CTBN 20-64.

B. Cleavage Testing

Seven flat plates of epoxy material, one for each of the above compositions, were cast between smooth glass plates using the standard cure and post cure procedures outlined in Appendix A. Tensile specimens were then machined from the smooth plate castings with geometries as shown in figure (3). It is imperative that the slot width be exactly 0.006 inch as erroneous tests results were obtained when this value was exceeded. The slot depth is also critical in that if the width of the material remaining exceeds one third the material thickness, it is likely the propagating crack will jump out of the slot resulting in erroneous values of fracture surface work.

The cleavage specimen was tested by inserting it in the Instron grips and conducting the test at a cross head

rate of 0.02 inch per minute. Various cross head rates were tried; however, at higher rates it was determined the material was very rate sensitive in that upon crack initiation, the crack would propagate the entire length of the specimen at a fast growth rate. This resulted in insufficient data for test analysis. The crosshead rate selected gave the most satisfactory results for the material tested.

The unmodified EPON 828 specimens left no permanent record of crack propagation and required marking points of crack arrest on the specimen with a felt tipped pen during the testing of the material. The specimen containing CTBN left a permanent record of crack length in that points of crack initiation and arrest were stress whitened whereas regions of rapid crack growth maintained the color of the bulk material.

Analysis of the test data to determine the fracture surface work, γ, was accomplished utilizing the cleavage technique of Broutman and McGarry (14) as outlined in Appendix D.

C. Uniaxial Tensile Testing

The materials for the tensile specimens were first cast and machined as described in Appendix A. The geometry of the tensile specimen was as shown in Figure (4). Uniaxial tensile tests were conducted on the seven material compositions as outlined previously, using the Instron testing machine at a cross head rate of 0.1 inch per minute.

D. Biaxial Stress Testing

A series of approximately twelve biaxial tensile cylinders were cast and machined utilizing the material composition of EPON 828 - 5% curing - 10% CTBN 151 W. This test data was used to supplement the study conducted by Oien (15). A series of approximately ten biaxial compressive cylinders were cast and machined for each of the first three compositions as specified in this introduction. Processes and techniques for producing these biaxial specimens are outlined in Appendix B.

In order to arrive at a satisfactory specimen geometry for the biaxial compressive cylinders, it was necessary to apply a trial and error solution. The geometry of these specimens required that they not be subjected to buckling prior to yielding. To satisfy this requirement, the biaxial tensile cylinder geometry was altered. The length of the cylinder was reduced by 1 1/2 inches to a final length of 4 1/8 inches with the cylinder thickness remaining at 1/16 inch. Upon testing this specimen, buckling occurred prior to yielding. A solution to this problem was achieved by increasing specimen thickness to 3/32 inch and testing resulted in buckling occuring after the specimen yielded. Thus a satisfactory biaxial compressive specimen geometry was derived from a trial and error solution.

Prior to the testing of these specimens the Instron testing machine was calibrated. The next step was to measure

the inner and outer diameter of the gage length of the specimen with a micrometer just prior to inserting the specimen in the specially designed Instron grips.

Each cylinder was tested to yielding or fracture using one of the following test procedures:

1. Instron tension only, at 0.005 inch per minute crosshead rate to a tensile force where the load vs. time, as plotted by the Instron chart, is of zero slope or the specimen fractures. This tests yields the tensile yield stress, 6_t.
2. Hydraulic pressure only, with no applied Instron tensile or compressive load. Pressure is increased slowly by adjusting the nitrogen cylinder air regulator valve until the specimen yields or fails in fracture. This test yields the hoop stress, 6_h, at which yielding occurs.
3. Instron compression only, at 0.005 inch per minute crosshead rate to a compressive force where the load vs. time, as plotted by the Instron chart, is of zero slope or the specimen fractures. This test yields the compressive yield stress, 6_c.
4. A combination of Instron tension or compression and hydraulic pressure which yields various

combinations of 6_t or 6_c and 6_h, defining the yielding envelopes.

In these tests, the ratio of the biaxial stresses is a constant. It has been found (16) that varying this ratio during the test on epoxy materials can severely reduce the fracture stresses. This reduction in strength can be attributed to the effects of creep. This ratio is maintained throughout the test until the specimen fractures or the slope of load vs. time is zero.

E. Uniaxial Compressive Testing

The materials for the compressive specimens were machined from the smooth plate castings of the first three compositions as outlined previously. The geometry of the specimens as shown in Figure (7) was derived from previous work performed by Bowden and Jukes (11 and 12). The critical dimension was the specimen height which is limited such that buckling will not occur prior to yielding. The compressive tests were conducted on these specimen at an Instron crosshead rate of 0.02 inch per minute.

F. Optical Microscopy

A Reichert optical microscope was used for examination of cleavage and biaxial specimen fracture and yield surfaces using a reflected light source due to the opaqueness of the material. Optical micrographs were recorded using a Polaroid camera.

G. Electron Scanning Microscopy (ESM)

Fracture surfaces of cleavage and tensile specimens were cut and prepared as outlined in Appendix C. The prepared specimen was inserted into the vacuum chamber of a Japan Electron Optics Laboratory Company, Ltd. (JEOLCO), type JSM electron scanning microscope. Standard JEOLCO operating instructions were followed in recording micrographs with a Polaroid camera.

H. Electron Transmission Microscopy

Two stage replication samples were prepared of each type of CTBN casting as outlined in Appendix C. The samples were viewed with a Phillips 100C electron transmission microscope, and micrographs recorded using a 35 mm camera.

CHAPTER IV

Experimental Results and Discussion

A. Effects of CTBN Elastomer Variation on Fracture Surface Work and Ultimate Tensile Strength

1. Introduction

It is acknowledged that there is a wide range of interaction of many factors such as the molecular weight, acrylonitrile content, particle size, temperature, type of curing agent used, and so on. Therefore, it is very difficult to separate these effects and study them alone without taking into account the effects of the others at the same time. Thus for the purpose of this study, it was attempted to only vary the first three of the aforementioned parameters to find the relationship between fracture surface work and ultimate tensile strength as the CTBN elastomer is varied in the matrix.

2. Experimental Results

The computed data for the ultimate tensile strength vs. CTBN composition is shown in Table II and graphically plotted in Figure (8). The data was arrived at by testing the uniaxial tensile specimens in the Instron testing machine, then determining the ultimate tensile strength by dividing the load force at yield by the original cross sectional area of the guage length of the specimen. This study revealed that the maximum ultimate tensile strength is achieved by utilization of unmodified EPON 828 or CTBN 20-64 (small

particles) modified EPON 828 which was the expected results (8, 15); however, by various combinations of CTBN 151 W (large particles) and CTBN 20-64 (small particles) modifying the epoxy matrix, it was possible to improve the ultimate test strength by approximately 15% over that of CTBN 151 W modified EPON 828. Previous results (15) had noted the significant loss of ultimate tensile strength in order to maximize toughness. Later results will show how the significant loss in strength is not necessary in order to improve the toughness of the material.

It was observed microscopically that in the case of the unmodified epoxy tensile specimen the fracture surface was very rough and contained a rather significant flaw as depicted by Figure (18) from which failure of the specimen initiated. This same specimen showed only a slight amount of necking of the gauge length prior to failure. All tensile specimens containing elastomer particles were observed through the electron scanning microscope to have a flaw or imperfection on the fracture surface from which inumerable, long, thin, white striations digressed radially (Figures 16 and 17). A scanning electron micrograph of the fracture surface of a tensile specimen composed of EPON 828 modified with CTBN 151 W (large particles), Figure 19, exhibits the rather rough fracture surface with an inumerable amount of voids and lesser number of particle inclusions. It may be the result of the large number of voids which leads to a

lower ultimate tensile strength for the large particle, CTBN 151 W, modified epoxy matrix. Shown in the same figure is a micrograph of a single CTBN 151 W elastomer particle whose halo effect is due to the gold shadowing of the specimen. The stressed particle has assumed a spherical shape and appears to have no crazes linking with it.

Specimens containing CTBN 151 W (8%) and CTBN 20-64 (2%) were noted to have necked rather severely and became milky white in appearance throughout a portion of the gauge length. The relative engineering strain of these tensile specimens utilizing the change in cross sectional areas approximated 22% at fracture. To determine the strain of several other tensile specimens, the Instron extensometer was utilized, however, the data obtained from this apparatus was incomplete for it was limited to strain measurements of 5%. The majority of material tested exceeded a yield strain of 5% but was less than 15% except for the aforementioned material.

The test data for the cleavage specimens was processed using the analysis techniques described in Appendix D. The values of fracture surface work determined for the seven material compositions is presented in Table I and graphically plotted in Figure 9.

The inclusion of CTBN 151 W and 20-64 elastomer particles in the ratio of 4:1 by weight respectively within the EPON 828 matrix increased the fracture surface work of

the modified material by nearly an order of magnitude over that of unmodified EPON 828, whereas CTBN 20-64 elastomer inclusions (small particles) were much less effective. The other compositions as viewed graphically in Figures (9) were almost as effective in increasing the fracture surface work as the first mentioned composition.

The seven materials are here ranked in order of decreasing fracture surface work or fracture toughness with respect to the elastomer inclusions:

R 151 W (8%) + 20-64 (2%)

R 151 W (6%) + 20-64 (4%)

R 151 W (4%) + 20-64 (6%)

R 151 W (2%) + 20-64 (8%)

R 151 W (10%)

20-64 (10%)

EPON 828 (Unmodified)

All cleavage specimens tested except unmodified EPON 828 and cleavage specimen 128 exhibited stress whitening in regions of slow crack propagation and a mirror-like smooth fracture surface in regions of fast crack propagation. This appearance of colors is thought to be proof that an oriented layer of molecules is present at the fracture surface (14). This fracture behavior is shown in Figure (15) which represents the transition between fast and slow crack propagation for four of the materials investigated. Of particular interest is the varying manner in which transition

is defined as the composition of the material is changed. In the case of unmodified epoxy, the fracture surface was mirror-like which indicates this material achieved the highest crack velocity of the cleavage tests conducted. The three other micrographs of Figures (15) show the varying degree of roughness of each of the fracture surfaces. From previous work (14), it has been shown that the material with the less roughened surface has a lower fracture surface work (toughness). Utilizing this analysis on the micrographs, the EPON modified with CTBN 20-64 (10%) has the least toughness and that modified with R 151 W (8%) and 20-64 (2%) has the greatest toughness which was precisely what the calculated results determined. Thus it can be seen how the micrographs present a somewhat relative picture of the material toughness. Referring now to cleavage specimen #128, it was rather unique in that it failed in a continuously tearing manner by slow crack propagation until the test was terminated, whereas all other cleavage specimens failed in a discontinuous manner.

Utilization of the scanning electron microscope with its higher resolution than the optical microscope reveals in much greater detail the cleavage specimens fracture surface as shown in Figures (20-22). The transition zone micrograph of Figure (20) shows very clearly the "river markings" of the slow crack propagation area and how they are elongated from right to left in the direction of propaga-

tion of the fracture (17). In this same figure, the slow crack propagation micrograph shows the tearing effect and slow crack velocity which is the means of fracture in this area, whereas the fast crack propagation micrograph displays a smoother surface and faster crack velocity. The micrographs of Figures (21 and 22) give a good characterization of the fracture surface of a material with a high degree of toughness. The fracture surfaces of these materials display a large degree of roughness, a great deal of color contrast, sufficient amount of stress whitening, and a fairly even distribution of particles and voids.

The toughening ability of the second phase rubbery particles may be understood more clearly by an interpretation of Figures (27 and 28) depicting the particle size and morphology of three representative CTBN modified epoxy materials. These materials were all cured with 5 pph of curing agent D at a temperature of 120°C then post-cured for two hours at 130°C. The factors which were varied included the molecular weight, acrylonitrile content, and particle size. The micrographs are shown at two different magnifications so that particle distribution can be readily visualized. In Figure (27), the micrographs show an average particle diameter of 555Å for CTBN 20-64 modified epoxy, 3,380Å for CTBN 151 W modified epoxy, and for the combination of CTBN 151 W (8%) and CTBN 20-64 (2%) a size range of 13,300Å to 3320Å. It is evident from these micrographs that a low

molecular weight and high acrylonitrile content results in small particle sizes, whereas the converse results in large particle size formulation. The most significant results of these micrographs is realized from the extremely large particles that are developed when the CTBN elastomers are utilized in combination, which previous results has shown these materials to have a superior toughness. It appears that a favorable interaction of molecular weight and acrylonitrile content is established which results in optimizing the toughening ability of the EPON/CTBN material.

3. Discussion

The experimental results obtained from the cleavage specimens show that unmodified EPON 828 which fractures with low surface energy can be fracture toughened by inclusions of second phase elastomer particles in EPON 828 matrix. However, in order for any significant improvement in toughening to take place, good bonding between the CTBN elastomer particles and the epoxy matrix is needed. A mechanism by which these particles improve the fracture properties of the thermosetting resin is by increasing the size of the plastic zone ahead of the crack, thus relaxing the high stress concentration which will otherwise exist at the tip of a crack (8). These particles also increase the energy to fracture by promoting the formation of voids.

The summary of results presented in Tables I and II show that the inclusion of strictly large elastomer particles,

low acrylonitrile content in EPON 828 greatly increases fracture toughness but reduces ductility and strength with respect to unmodified EPON 828. The inclusion of strictly small elastomer particles resulted in slight improvement of fracture toughness but much improved strength property with regards to unmodified EPON 828. When the two different elastomers were mixed together in various combinations, the fracture toughness became superior to any of the individual elastomer additive compositions. In addition, favorable improvement in the strength property was observed with respect to the epoxy matrix modified by large elastomer particles.

It is reasoned that by combining elastomer particle sizes in a constant CTBN elastomer concentration of 10% by weight, the optimum toughening of the epoxy matrix can be achieved, yet not sacrifice appreciable strength. The properties obtained appear to be due to an interaction of the molecular weight, acrylonitrile content, and particle size of the various CTBN elastomers. The interactions which take place resulting in this optimization may be hypothesized in the following manner. The amount of reaction and polymerization of CTBN with epoxy molecules is dependent upon carboxyl groups only. The lower the carboxyl group's density is, the fewer are the epoxy - CTBN reactions that can take place. The density of the carboxyl group is defined here as the ratio of the number of carboxyl groups present on one

butadiene - acrylonitrile chain molecule over the molecular weight of the molecule. Thus changing this ratio will affect the cross-linking density inside the particles and the amount of reaction and polymerization with epoxy molecules. In addition, the mutual compatibility of CTBN with epoxy increases as the molecular weight of CTBN increases. Thus the chemical and mechanical bonding of the particles with the matrix is increased as the particle size increases.

With respect to the tensile strength, the difference in coefficients of expansions between the glassy phase of EPON 828 and the elastomer particles can create tension in the rubber particles (3). The epoxy is then under a tangential compression; reducing the stress produced by an external load and drastically altering the maximum shear stress at the particle-matrix interface. From the test results, it appears that the large elastomer particle inclusions reduce the specimen strength most severely by means of the above hypothesis and that small elastomer particle inclusions are least effective in reducing strength.

B. Effect of CTBN Elastomer Particle Size on Yield Criteria For Plastic Deformation of Glassy Polymers

1. Introduction

Experimental evidence appears to indicate that the biaxial yield of many ductile metals and plastics can be predicted to a good approximation, using the von Mises criterion (9 and 11). The Tresca criterion has also been

found to give reasonably good results, although not quite as accurate or dependable. Both of these theories have a possible shortcoming in that they make no distinction between the yield strength in tension and a possible different value of yield strength in compression. While there are many materials for which these values are almost identical, such as polymethylmethacrylate, there are also some materials for which they are significantly different, such as some epoxy resins. At the present time there are no clear cut rules for predicting which theory of yielding will apply to a given polymer. In terms of materials, the picture is even less clear since we have, at present, only an elementary quantitative understanding of the relationships between failure phenomena and microstructures. Thus the purpose of this study was to investigate the yield behavior of a glassy polymer under a system of biaxial stress in an attempt to define a criterion for yield. By subjecting unmodified and elastomer modified epoxy samples to a biaxial stress field, it is possible to obtain yield envelopes which are indicative of the modes of failure taking place. Electron microscopy of yielded and fractured biaxial specimens is also useful in determining the flow mechanisms which are taking place during yield or fracture. In glassy polymers two distinct modes of plastic deformation have been identified, namely normal stress yielding (crazing) and shear yielding.

2. Results From Biaxial Tensile Tests

Previous work (15) conducted on biaxial tensile specimens is plotted in Figures (10-12). It was concluded by Oien (15) that biaxial tensile specimens of EPON 828 (unmodified) and CTBN 20-64 yielded in a ductile manner exhibiting the shear yielding criterion of von Mises with no macroscopic evidence of stress whitening, crazing or void formation. Specimens of CTBN 151 N, consisting of large elastomer particles, did not generate a von Mises type yield envelope but suggested rather a cusped shaped curve. This cusp shaped curve was considered to be similar to the craze yielding curve for PMMA (11) and strongly suggested that the material fails in a tensile manner and is brittle. A recent interpretation of this data by McGarry and Sultan agreed with the conclusion that a cusp form similar to that of the crazing yield envelope for PMMA (9, 12) was appropriate for the CTBN 151 modified epoxy; however, they further concluded that the form of the envelope suggests that a Tresca maximum shear criterion may also be valid in this case.

An additional twelve biaxial tensile specimens composed of CTBN 151 W modified epoxy were tested and the results plotted in Figure (10) and tabulated in Table IV. It is evident from the plot of the test data that a cusped shape curve does not fit the data, but that a Tresca maximum shear criterion envelope fits the data most appropriately. In Figure (14) is shown a fractured biaxial specimen composed

of CTBN 151 W modified epoxy which has been subjected to a very high hoop tensile stress. This fracture surface reveals that the material when subjected to high tensile stresses will fail by brittle fracture before ductile yielding can occur. A typical yield surface for the aforementioned material is shown in Figure (24). Analysis of the appropriate yield criterion will be discussed in more detail later.

3. Results From Compression Tests

A number of castings of the three compositions utilized for this study fractured as a result of thermal stresses built up in the material due to the mold cooling rate being excessive. The results of this failure can be viewed in Figure (13). In order to curtail the thermal stress effect, it was necessary to double the wall thickness to 1/4 inch for the outer mold sleeve, thereby a more even and controlled rate of cooling was realized by the casting. The results of this mold design change permitted satisfactory material castings to be manufactured without excessive thermal stresses.

The results of the tests of compression specimens are tabulated in Tables V-VII. These resultant values for 6_c and 6_h were determined using stress formulas for an open ended cylinder (18). The axial compressive stress, 6_c, is derived from the formula:

$$6_c = \frac{F}{A}$$

where,

F = Instron compressive load

A = Cross sectional area of guage material perpendicular to the compressive axis.

The resultant values for hoop tensile stress, 6_h, in an open ended cylinder are derived from:

$$6_h = \frac{Pr}{t}$$

where,

P = Hydraulic fluid pressure

r = Mean cylinder wall radius

t = Cylinder wall thickness

This data was then used to obtain the graphical results shown in Figures (10-12).

The shear yield stresses of all these materials were pressure-dependent. Figures (10-12) show plots of the compressive yield stress, 6_c as a function of hoop tensile stress, 6_h, and it can be seen that the slope of the best fit straight line through the experimental data points is in all cases greater than 45°. In addition, all the materials tested showed a load - time curve with an upper yield stress followed by a load drop.

Sections were cut from a deformed specimen of each of the materials and examined through a Reichert optical microscope using reflected light. The optical micrographs of the yield surfaces of the biaxial compressive specimen are shown in Figure (23). Of the materials tested EPON 828 (unmodified) and EPON 828 modified by CTBN 20-64 (small

particles showed broad difuse regions of deformation, whereas EPON 828 modified by CTBN 151 W (large particles) contained smooth, thin well defined regions of deformation. CTBN 151 W modified epoxy also in some cases showed regions of high local shear strain referred to as shear bands that are shown in the yielded biaxial compressive specimen in Figure (14). For a material that forms well-defined shear bands, a Tresca criterion is to be expected (19). The bands always formed on planes inclined at less than 45° to the compression direction. The fracture surfaces of CTBN 151 W modified epoxy biaxial compressive specimens exhibited significant whitening and void formations as seen in Figures (25, 26) which indicates that the CTBN 151 W particles promote this behavior through mechanisms dependent upon particle size. It is therefore reasoned that a threshold of particle size exists above which the behavior exhibited by CTBN 151 W is promoted.

4. Discussion - The Yield Criterion

Considering the large compressibility of polymers, an attractive hypothesis is that the yield stress is controlled by molecular chain segment mobility which is in turn directly related to the hydrostatic component of the applied stress system (12). This idea has been well expressed by Sternstein and Ongchin (9) who propose essentially a von Mises criterion for yield $[(6_c - 6_h)^2 + (6_h - 6_3)^2 + (6_3 - 6_c)^2 = 6K^2]$ with the value of the constant K varying linearly with

hydrostatic pressure, $K = K_o + \mu P$. P is the compressive hydrostatic component of the stress system and μ is a constant that will be referred to as the coefficient of internal friction. Another possibility is a Tresca yield criterion [$|6_c - 6_h| = 2K$] with the constant K again pressure-dependent.

At the yield point the material is flowing viscously and the applied stresses are constant. The strain rate in a direction perpendicular to 6_c and 6_h must be zero and Nadai has shown (20) that if this is the case then the component of the deviatoric stress tensor in this direction (the 6_3 direction) must be zero. It follows that $6_3 = 1/2 (6_c + 6_h)$. Using this relation it can be shown that both the criteria above predict that 6_c vs. 6_h plots in Figures (10-12) will cut the axes at:

$$6_c = -\frac{2K_o}{1-\mu} \text{ and } 6_h = \frac{2K_o}{1+\mu}$$

Consequently values of both K_o and μ can be derived directly from the plots in Figures (10-12). For the two criteria, the predicted ratios of the compressive yield stress in plane strain to the unconstrained compressive yield stress are $2(\sqrt{3} - \mu)/(3(1-\mu))$ (von Mises) and $(3-2\mu)/(3(1-\mu))$ (Tresca). To complete this method of analysis, the experimentally determined value of the ratio must be determined. The calculated values derived using this analysis method and the data plotted in Figures (10-12) is shown in the below table.

Material	Ko	μ	von Mises Ratio	Tresca Ratio	Experimental Ratio
EPON 828	5.872	.068	1.19	1.025	.956
CTBN 20-64 Mod.	5.265	.043	1.72	1.012	.895
CTBN 151 W Mod.	4.809	.118	1.22	1.045	.99

From the data presented in the table, it is apparent that the experimentally determined ratio does not appropriately indicate either a Tresca or a von Mises yield criterion is applicable to the yielding of these materials in compression. It is further realized that the utilization of the hypothesis developed by Bowden and Jukes (12) for determining the criterion for yield of a glassy polymer is not a satisfactory means of analysis for these materials. This shortcoming is partially due to the yield stress in uniaxial compression exceeding the yield stress in plane-strain compression in each material tested.

It is apparent at this stage of the analysis of the data presented in Figures (10-12) that in order to arrive at any satisfactory conclusion with regards to establishing a general yield criterion, that the data should be analyzed as one entity and not as two separate unassociated quadrants. Previous studies (9, 10, 11, 12 and 15) have based their yield criterion analysis on either the first quadrant or the second quadrant but not both quadrants together. Future work should be devoted to testing in both quadrants simultaneously in order to achieve a more indicative set of data for interpretation as to the appropriate yield criterion

for the material being tested. It still remains feasible that the data determined may appear to be in general agreement with one yield criterion in the first quadrant and with another yield criterion in the second quadrant.

Further analysis of the data was performed using Mohr's circle construction congruent with Coulomb's yield criterion as shown in Figure (12b). Construction of the Mohr's circles utilized the data presented in the second quadrant of Figures (10, 11 and 12). Each point for which ductile yielding occurred defines a circle on the Mohr's circle diagram, and the envelope of these circles defines the straight line labelled "yield surface" in the figure.

On this criterion, the critical shear stress for yielding to occur on any plane in the material increases linearly with the pressure applied normal to the plane. The critical shear stress can be written

$$S = K_o + \mu P$$

where K_o = cohesion of the material

μ = coefficient of internal friction

P = normal pressure on shear plane.

In this analysis the yield-point has been defined as the point at which non-recoverable and therefore plastic strains are produced in the specimen, and the criterion for yielding in plane strain has been determined in terms of the applied stresses. This criterion can be specified not only as a function of 6c and 6h, but also as a pressure-

dependent shear yield stress. The criterion can be stated: the material will yield when the shear stress on any plane reaches a value given by $S = K_o + \mu P$, and yield will occur in shear on this plane.

Further analysis as exhibited in Figures (10a, 11a and 12a) revealed that a "modified" Mohr-Coulomb criterion was in general agreement with the data presented in both quadrants for the unmodified EPON 828 and the epoxy modified with small elastomer particles. The deviation of the data for the large particle modified epoxy material with the application of this criterion led to its rejection and the acceptance of the prior suggestion that a Tresca maximum shear criterion appears to be valid in this case due to the form of the yield envelope in the first quadrant. Further testing is required to fully justify the applicability of the Tresca criterion.

The behavior of unmodified EPON 828 and small elastomer particle modified epoxy under a biaxial stress field as shown in Figure (11a and 12a) reveals a drop in yield strength when subjected to a biaxial tension and suggests that these materials follow a "modified" Mohr-Coulomb cirterion. If P and T_{OCT} are the mean normal and octahedral shear stresses acting on a plane, this criterion states that yielding or fracture takes place for the plane on which the magnitude of T_{OCT} first becomes equal to $(K_o + \mu P)$:

$$T_{oct} = K_o + \mu P$$

where, K_o = pure shear yield stress

$$= 1/3 \sqrt{(6_1-6_2)^2 + 6_1^2 + 6_2^2}$$

μ = coefficient of internal friction (compute value for each quadrant)

P = mean normal stress

$$= \frac{6_1 + 6_2 + 6_3}{3} \quad \text{where } 6_3 \simeq 0$$

Sternstein and Ongchin (9) found similar results for the shear yielding of glassy PMMA in the first quadrant.

The calculated values derived using this analysis, $T_{oct} = K_o + \mu P$, and the data plotted in Figures (10a, 11a and 12a) are shown in the table below.

Material	Quadrant 1		Quadrant 2	
	K_o	μ	K_o	μ
EPON 828	6,050	.310	5540	.096
EPON 828 + CTBN 20-64	5,500	.380	4970	.062
EPON 828 + CTBN 151W	4,460	.139	4550	.165

CHAPTER V

Conclusions

The purpose of this research was twofold. It was an attempt to find a method of optimizing the toughness of elastomer modified epoxy resins without significantly sacrificing material strength. The method selected was to toughen an epoxy matrix by the inclusion of various elastomer particles in combinations not to exceed 10 pph. The second purpose of this study was to investigate the yield behavior of modified and unmodified epoxy under a system of combined stress in an attempt to define a criterion for yield. On the basis of the work completed, the following conclusions appear valid:

1. This study has determined the fracture surface work and ultimate tensile strength, Figures 8 and 9), of several Hycar CTBN/epoxy resin compositions. The Hycar CTBN liquid polymers are additive to the epoxy resin and were prepared especially to show the importance of molecular weight, acrylonitrile content, and particle size in optimizing for tougher thermosetting polymers.

   It is concluded that by combining two different elastomers in a constant CTBN elastomer concentration of 10% by weight, the optimum toughening of the epoxy matrix can be achieved and yet not sacrifice appreciable strength and

ductility of the material. The properties obtained appear to be due primarily to an interaction of the molecular weight, acrylonitrile content, and particle size of the various CTBN elastomers. In addition, good bonding between the CTBN elastomer particles and the epoxy matrix was required in order to realize any significant improvement in material toughening. It is hypothesized that the optimum toughening of the matrix is achieved through the flexibility of the molecular network. The improved ultimate tensile strength is a result of the mutual compatibility the respective CTBN elastomers have with the epoxy in regard to the stress concentrations they establish with the particle matrix interface.

2. Using electron microscopy to study the morphological features of the various epoxy/elastomer formulations proved to be a critically important element in the research, permitting correlations between microstructures of the formulations and their microscopic behavior in a manner impossible by other means. The morphological parameters observed were particle size, particle size distribution, and volume content of precipitated particles.

Morphologically it is observed, Figure (23), that a precipitated second phase is significantly effective in toughening the material only if the particle size is above a minimum diameter of ∿3,000 Å. In addition, the effectiveness of the second phase increases as the size of the particle increases. The size of the precipitate particles can be increased by:

a. increasing the molecular weight of the elastomer, CTBN.

b. decreasing the acrylonitrile content of the elastomer, CTBN.

c. using elastomers in combination to modify the epoxy matrix.

d. using Curing Agent D.

e. using a high cure temperature, ∿120C.

3. The yield behavior of modified or unmodified epoxy under a biaxial compression stress system failed to follow the criterion for yield as hypothesized by Bowden and Jukes (12). This failure to appropriately approximate either a von Mises or Tresca yield criterion in the second quadrant is concluded from the graphical results shown in Figures (10-12) and is also due to the fact that for these materials the uniaxial compressive yield stress exceeds the

plain-strain compressive yield stress, thereby preventing a favorable comparison of the ratios of plain-strain compression to uniaxial compression.

4. In order to establish a general yield criterion, it is recognized that test results should be presented simultaneously for both the first and second stress quadrants. It appears that by analyzing each quadrant individually, erroneous conclusions may be derived. It is recommended that future studies consider the analysis of both quadrants simultaneously to arrive at any conclusions regarding a yield criterion for the material under investigation.
5. The shear yielding behavior of modified and unmodified EPON 828 under a biaxial stress system is exhibited in Figures (10-12a). Analysis of these results concludes that the shear yielding of these materials with exception of the epoxy modified with large elastomer particles in the first quadrant is most consistent in terms of a Mohr-Coulomb yield criterion. The criterion can be stated: the material will yield when the shear stress on any plane reaches a value given by $S = K_o + \mu P$, and yield will occur in shear on this plane.

Examination of epoxy with CTBN 151W, exhibited in Figures (10 and 10a), which produces large second-phase particles implied that there are two distinctly different yield criteria involved. From the microscopic and graphical results, it is concluded that a Tresca maximum shear criterion appears to be most valid for this material in the first quadrant and a Mohr-Coulomb criterion most appropriate in the second quadrant. Further testing is necessary to validate the Tresca yield criterion for this material in the first quadrant.

CHAPTER VI

Recommendations for Future Work

The present thesis work emphasized the possibility of optimizing the fracture surface of thermoset resins. It was shown that the incorporation of second phase, elastomer particles in various combinations in the polymeric matrix increases the fracture surface work of these materials. In addition, a better understanding of the yield criterion appropriate to epoxy resins and elastomer modified epoxy resins has been realized.

Although the experimental work of this thesis has answered a few questions, it also has created a large number of questions which remain to be answered regarding the behavior of elastomer particles in stressed glassy polymer matrix material. Some of the most important questions to be treated in depth should include:

1. The activation energy should be determined for modified and unmodified epoxy to evaluate the yield criterion involved.
2. Further study into the mechanism of shear band initiation and the influence of the rubber particles is required. Experimental evidence supports the use of very low acrylonitrile elastomer particles for this study.
3. A microscopical study of the formation of voids,

crazes, and shear bands and conditions favoring their respective development.

4. Further study of the elastomer particle sites is needed to determine how they act as stress concentrators and what effects they supply with respect to residual thermal stresses.
5. A careful examination of which mechanism forms crazing and which mechanism promotes shear banding should be pursued in more detail. In addition, the relationship of stress whitening and particle deformation to material toughening requires further investigation.
6. To better understand the toughening process, the molecular mechanism of yielding must be further defined.
7. In general, a better understanding of the relationships between failure phenomena and microstructure is required.

REFERENCES

1. McGarry, F. J., Willner, A. M., and Sultan, J. N., "Effects of Interstitial Inclusions in Fiber Reinforced Composites," MIT, Technical Report AFML-TR-69-86, May, 1969.

2. Bucknall, C. B. and Smith, R. R., "Stress Whitening in High Impact Polystyrene," Polymer, 6, 1965.

3. Andrews, R. D., Jr., Allison, S. W., Ender, D. H, Kimil, R. M., and Whitney, W., "Research Study in Cold Drawing Phenomena in High Polymers," MIT School of Engineering, Technical Report 67-10-CM, Chapter IV, August, 1966.

4. Stegeman, F. C. and McGarry, F. J., "Relationship Between Resin Fracture and Composite Properties, Crack Propagation Behavior of Thermoset Resins Containing Polyethylene Microparticles," First Quarterly Report, Contract AF 33(615)-2712, Materials Research Laboratory, Civil Engineering Department, MIT, September, 1965.

5. Sultan, J. N. and McGarry, F. J., "Toughening Mechanisms in Polyester Resins and Composites," Research Report R67-66, MIT, Cambridge, Mass., December, 1967.

6. McGarry, F. J., Willner, A. M., and Sultan, J. N., "Relationship Between Resin Fracture and Composite Properties," Technical Report AFML-TR-67-381, MIT, December, 1967.

7. Sultan, J. N. and McGarry, F. J., "Microstructural Characteristics of Thermoset Polymers," Research Report R69-59, MIT, Cambridge, Mass., 1969.

8. Sultan, J. N., "Criteria in Toughening Thermoset Resins", Ph.D. Thesis, MIT, Civil Engineering Department, 1969.

9. Sternstein, S. S. and Ongchin, L., "Yield Criteria For Plastic Deformation of Glassy High Polymers in General Stress Fields," Polymer Preprints, Vol. 10, No. 2, September 1969.

10. Sternstein, S. S., Paterno, J., and Ongchin, L., "Stress Field Criteria For Yielding and Crazing of Glassy Polymers, and the Mechanism of Toughening in Rubber-Modified Systems," International Conference on the Yield, Deformation and Fracture of Polymers,

Cambridge, 1970.

11. Bowden, P. B. and Jukes, J. S., "Plastic Yield Behavior of Polymethylmethacrylate," Journal of Materials Science, 3 (1968) 183-190.

12. Bowden, P. B. and Jukes, J. A., "A Yield Criterion for Isotropic Polymers, Shear Band Formation and the Effect of Structure on the Yield Behavior," International Conference of the Yield, Deformation, and Fracture of Polymers, Cambridge, 1970.

13. Rowe, E. H. et al., "Liquid Rubber for Toughening Resins," B. F. Goodrich Research Center Publications, Brecksville, Ohio, 1969.

14. Broutman, L. J. and McGarry, F. J.,"Fracture Surface Work Measurements on Glassy Polymers by a Cleavage Technique," J. Appl. Polymers Sci., 9, pp. 589-608, (1965).

15. Oien, H. M., "An Investigation of Biaxial Stress in Rubber Modified Plastics," Naval Engineer Thesis, MIT, Naval Architechture Department, 1970.

16. Baer, E., Engineering Design for Plastics, Polymer Science and Engineering Series, New York, pp 277-399 (1964).

17. Andrews, E. H., Fracture in Polymers, American Elsevier, New York, 1968.

18. Crandall, S. H. and Dahl, N. C., An Introduction to the Mechanics of Solids, McGraw-Hill Book Company, Inc., Chapter IV, 1959.

19. Taylor, G. I., Proc. Roy. Soc. 145A, 1, 1934.

20. Nadai, A., Theory of Flow and Fracture of Solids, McGraw-Hill Book Company, 1950.

APPENDIX A

Cleavage and Tensile Specimen Casting and Machining

The casting and machining procedure for EPON 828, 10% CTBN and 5% Curing Agent D consists of the following sequence:

1. Prepare the mold by cleaning two 12" by 12" glass plates and then coating them with two coats of mold release, Frekote 33#, allowing at least ten minutes between coats for drying. A ¼ inch thick rubber gasket cut from a neoprene rubber sheet is also coated with the mold release.
2. The plates are then secured to the gasket with binder clamps. The mold and oven are preheated to 120°C and are ready for the liquid resin.
3. Measure the desired amount of EPON 828 on a balance in a clean, dry beaker.
4. Add the desired amount of CTBN to the EPON beaker.
5. Place the beaker in a mineral oil bath at 275°F insuring that the bath liquid level is above that of the EPON-CTBN level in the beaker.
6. Stir the EPON-CTBN mixture with a steel spatula as it is heated in the oil bath. Leave the mixture in the bath until the solution is fully transparent and all surface and subsurface bubbles and froth

have disappeared. This process takes approximately 20-30 minutes.

7. The mixture is then deaerated in an evaporator for approximately fifteen minutes. The mixture must be hot for positive results. (Delete for unmodified EPON 828)
8. Place the beaker back in the oil bath and heat until no bubbles exist or until the solution is at 250°F. If bubbles persist, resume evaporation. Always reheat the solution after evaporating process.
9. Remove the beaker from the oil bath and place on the balance. Allow the solution to cool with occasional stirring until a thermometer reading of 100°C is obtained. (80°C for unmodified EPON 828)
10. Remove the mold from the oven and place on a table ready for pouring of the mixture.
11. Add the desired amount of Curing Agent D to the EPON-CTBN mixture and stir thoroughly until the mixture is entirely homogeneous.
12. Pour the mixture into the preheated mold. Place the mold in the oven and cure at 120°C for two

hours, after which the plate casting is allowed to cool to 50°C and is then post cured at 130°C for two hours and allowed to cool to room temperature in the oven.

13. The castings is removed from the mold, and then machining of the specimens is accomplished using a band saw and a small milling machine. The specimens are machined to the measurements of Figures (3) and (4).

14. The cleavage specimens are then drilled using a special jig with predrilled 0.125" diameter holes. Then the slots were cut with a circular rotary saw with a 0.006 inch tooth radius. It is most important to cut the slot so that only precisely one-third the specimen thickness remains. After the sides are slotted, a crack ("swallow tail" cut) about 1 inch in length is machined at one end of the specimen.

15. The tensile specimens are machined on the milling machine using a special wishbone jig in which the specimen is inserted and secured. It is then slowly milled to size, insuring that too large a

cut is not taken, thus preventing the specimen from being gouged and ruined.

APPENDIX B

Biaxial Specimen Design, Casting, Machining, and Testing Apparatus

A. Biaxial Specimen Design

Specimen geometry is a compromise of various design factors as discussed in references (9, 10 and 15). A radial stress gradient is produced by internal hydraulic pressure, creating higher stress on inner wall areas than the ambient pressure stress on the outer wall. This radial stress gradient, 6_3, is minimized by achieving a small ratio of wall thickness to mean specimen diameter, less than 1:10 ratio (16). According to Crandall and Dahl (18) and Nadai (20), the radial stress, 6_3, is considered to be negligible in that, $\frac{t}{r} << 1$. The biaxial specimen must withstand the tangential hoop stress induced by internal pressure and Instron tensile/compressive stress applied parallel to the cylinder axis. The tangential hoop stress also varies from the inner to outer surface and its variation is again minimized by a small thickness to mean diameter ratio. The thickness of the compressive specimens also must be sufficient to eliminate bucling effects prior to specimen yielding. These desirable factors are countered by a requirement to minimize material shrinkage stresses created during casting

and curing of specimens and maintaining experimentally applied stresses within the capacity of the pressure system and tensile tester.

An estimate of maximum tensile, compressive and hydraulic forces necessary for testing specimens of this geometry was determined using EPON 828 ultimate tensile strength of 10.17×10^3 lb./in.^{2} and considering the specimen to be an opened cylinder. The anticipated maximum forces were estimated to be:

Instron tensile force	F axial = 2,000 lbs.
Instron compressive force	F axial = 4,600 lbs.
Hydraulic pressure	$P_{hyd.}$ = 1,400 psi.

These forces were considered obtainable with specimen geometry of figures (5 and 6).

The design of the specimen casting molds consisted of two pieces of stainless steel pipe and an aluminum spacer. The inner mold pipe or barrel required a highly polished surface with outside diameter of 1.250 inches and a length of 6.50 inches. The outer mold pipe or sleeve was unpolished with inside diameter of 2.00 inches, minimum outside diameter of 2.50 inches, and a length of 7.00 inches. The aluminum spacer was sized to give a snug fit with barrel and

sleeve and to space them concentrically, forming a 0.375 inch casting wall thickness.

B. Biaxial Specimen Cylinder Casting

Two basic specimen material types were cast for biaxial testing, the first consisted of EPON 828 and Curing Agent D with the second consisting of EPON 828 modified with various CTBN's and Curing Agent D. Casting procedure for EPON 828, 10% CTBN, and 5% Curing Agent D consisted of the following sequence with the noted differences for unmodified EPON 828:

1. Measure the desired amount of EPON 828 on a balance in a clean, dry beaker.
2. Add the desired amount of CTBN to the EPON beaker.
3. Place the beaker in a mineral oil bath at 275^{o}F insuring that the bath liquid level is above that of the EPON/CTBN level in the beaker.
4. Leave the EPON/CTBN mixture in the bath until the solution is fully transparent and all surface and subsurface bubbles and froth have disappeared. This often takes 20-30 minutes. Stir frequently with a glass thermometer to insure a homogeneous blend.
5. Lightly polish the mold barrel with 000 grade steel

wool. Press the steel wool to barrel only lightly.

6. Wipe the barrel with a dry, clean, soft cloth to remove dust, steel wool and old Frekote 33* particles. Do not touch the barrel with oily hands; gloves are recommended.
7. Spray the barrel surface with a light coat of Frekote 33 release agent.
8. Place the barrel into the oven at 120°C for approximately 10 minutes.
9. Take the barrel from the oven and allow it to cool for approximately 10 minutes, then spray lightly with another coating of Frekote.
10. Remove old Frekote particles from the inner surface of the sleeve as any particles may become incorporated in the casting and will cause axial fractures in the material.
11. Spray the aluminum spacing ring and inner sleeve surfaces with a coating of Frekote.
12. Assemble the three mold components and place the assembly into the oven at 120°C for at least 15 minutes.

---

*Mold release agent mfg. by Frekote, Inc., Indianapolis, Ohio

13. When the EPON/CTBN mixture is clear and hot, degas the solution in a vacuum desiccator for 15 minutes. (Delete for unmodified EPON).

14. Place the beaker back in the oil bath and heat until no bubbles exist or until the solution is at 250°F. If bubbles persist, continue degasing. Always reheat the solution after degasing. (Delete for unmodified EPON).

15. Remove the beaker from the oil bath and place on the balance. Allow the solution to cool with occasional stirring until a thermometer reading of 100°C is obtained. (A reading of 80°C is required for unmodified EPON).

16. Remove the mold from the oven and place on a table ready for pouring of the solution.

17. Add the desired amount of Curing Agent D to the EPON/CTBN solution and stir slowly until the solution is entirely homogeneous.

18. Pour the solution into the mold.

19. Upon completion of filling the mold, take a round wooden stick and brush up and down around the periphery of the inner barrel. Do not press

heavily as this will remove Frekote and the hardened solution will stick to the barrel.

20. Place the mold in the oven and cure at 120°C for two hours, after which the sample is allowed to cool to 50°C and is then post cured at 130°C for two hours. It is then allowed to cool to room temperature in the oven.

21. The biaxial specimen casting is then removed using an arbor press.

C. Machining of Biaxial Castings

After removal from its mold, the casting is pressed onto an expanable mandrel and mounted in a turning lathe. It is extremely important that an indicator be used for lathe alignment prior to accomplishment of a machining process on the casting, insuring uniform specimen thicknesses. The casting is then turned to 1.875 inches outside diameter and the ends are squared off to give 5.625 inch tensile and 4.125 inch compressive cylinder lengths.

The cylinder is again mounted on the mandrel and one inch grip thread lengths are marked at either end. A round cutting head of 1 1/2 inch diameter is used to cut the gage region of the specimen to a central diameter of 1.365 inches

for a tensile specimen and 1.438 inches for a compressive specimen using a final pass cut depth of less than 0.005 inch. The biaxial specimen is then polished with 000 grade sandpaper or steel wool.

Final machining consists of threading both ends of the specimen with 10 threads per inch of 0.075 inch depth (minimum). A completely machined specimen is shown in figures (2,5 and 6) and is now ready for testing.

D. Biaxial Specimen Testing Apparatus

An Instron testing machine grip assembly designed and constructed by Oien (15) utilizing the experimental procedure of Sternstein and Ongchin (9) was used for this experimental work. Components of this assembly consisted of an upper grip, lower grip, stainless steel plunger with an adjustable length, three high pressure O-rings, and a plexiglass safety shield. A complete assembly mounted in the Instron testing machine is shown in figure (1).

The hydraulic fluid pressurizing equipment consisted of a nitrogen compressed gas cylinder and regulator valve; a one gallon capacity hydraulic accumulator unit; a hydraulic pressure gauge of 2,000 psi capacity; high pressure tubing, pipe connections and regulating valves; and Dow-

Corning 550 fluid (silicon fluid).

The entire system functioned as a unit with nitrogen gas being introduced into the bottom of the accumulator unit, inflating a rubber membrane which forces silicon fluid out the top of the accumulator, through a valve and hose to the lower Instron grip and then the interior walls of the specimen. The hydraulic (silicon) pressure was controlled by adjustment of the compressed nitrogen cylinder air regulator valve. Simultaneously with the operation of the hydraulic equipment was the operation of the Instron crossheads either applying an axial tensile or compressive stress. This experimental study maintained a fixed ratio of tensile/compressive load to hydraulic load throughout each individual biaxial test.

APPENDIX C

Sample Preparation Technique for Electron Microscopy

A. Transmission Electron Microscope Specimens

Bulk samples of the various formulations were polished using standard metallographic polishing techniques. This technique entailed utilizing four different size grits. As the sample is transferred from each grit, it is rotated 90^{o} to provide a smoother polished surface. The sample is then polished mechanically using alumina 1, alumina 2, and alumina 3 respectively as polishing agents. This technique permits the second phase particles of the samples being elastomeric in nature to be preferentially polished more than the matrix, thereby producing a surface topography that can be replicated for electron microscopic examination. A two stage replication technique was found to produce satisfactory results for this material. The steps utilized were as follows:

1. A dilute solution of polyvinyl alcohol (PVA) is cast on the polished surface and allowed to harden overnight. This initial coating of PVA is then removed with cellophane tape and a new coating of PVA placed on the polished surface. This insures

a clean surface for replication.

2. A small piece of lens paper is placed over the area of interest of the sample. Cellophane tape is placed over the lens paper, then the PVA is loosened around the edges with a razor blade. The tape is pressed down firmly, then gently lifted thus stripping the PVA from the sample. A new coating of PVA is then put on the sample to preserve the polished surface for reuse.
3. The PVA film is taped to a glass slide with the side which has been in contact with sample exposed.
4. The slide is placed in the vacuum evaporator and shadowed with chromium at about 45^{o} in about eight short bursts with a reading of eight on the heat control dial. An evaporator dish with a drop of oil in it is used to determine when a sufficient amount of chromium shadowing is achieved. The specimen is then backed with a thin layer of carbon.
5. The specimen is removed from the evaporator, and specimens small enough to be picked up on a 200 mesh copper grids are cut from the PVA/chromium/carbon/paper sandwich. The paper is removed with

tweezers, and the replica placed in a distilled water bath until the PVA has dissolved (5 hours). The remaining chromium/carbon replica is then scooped up on a copper grid and allowed to dry.

6. The replica is then placed in the electron transmission microscope for viewing.

B. Electron Scanning Microscope Specimens

Bulk samples of the various formulations are prepared for viewing in the following manner:

1. Sections are cut from the fractured surfaces of the test specimens. The section size is limited to 1/4 inch in height and a base not to exceed 3/8 inch diameter.
2. The specimen is mounted on a 3/8 inch diameter aluminum disk. A small strip of aluminum paint is then placed down two sides of the specimen.
3. The aluminum disk is then mounted on a flywheel of a small rotary motor. This apparatus is then mounted in the vacuum evaporator at 90° from the evaporator basket. About 1/2 inch of gold wire is then placed as a small ball in the evaporator basket.

4. The motor is placed in operation, rotating the specimen, thus insuring an even shadowing. The specimen is then shadowed with gold in five short bursts at low heat.
5. The specimen is removed from the vacuum evaporator and placed in a vacuum jar until it is viewed with the electron scanning microscope.

APPENDIX D

Fracture Surface Work Measurements By Cleavage Technique

The fracture surface work values of the various resin formulations were determined using the cleavage technique described by Broutman and McGarry (14). When a tensile force is applied to the drilled ends of the cleavage specimen shown in Figure (3), a previously initiated crack propagates down the central slot and the sample behaves as a pair of cantilevers, anchored at the unsplit end. Analyzing it as such, the fracture surface work, γ, is given by:

$$\gamma = \frac{nF\delta}{4wL}$$

where F = applied force

δ = deflection of one cantilever

w = crack width

L = crack length

n = experimental constant

The cleavage specimen is deformed at a constant cross-head rate of 0.02 inches per minute in an Instron Testing Machine and a trace of load vs. time is obtained on the chart recorder; the force and deflection are taken directly from this chart. The crack length is measured during propagation, and its width is precisely determined after

the test has been completed. The constant, n, is found from the slope of a plot of log (F/δ) vs. log (L) since $F = a^{\delta}/L^{n}$ for a cantilever, where a is a second constant. Once n is found, the value of γ can be calculated for each crack length in the specimen. The crack either runs smoothly (continuous tearing) or jumps two to four times (stick-slip tearing) before the specimen fails, so several determinations of γ are possible with each specimen. In some cases the γ value determined from the first or last jump is significantly different from the average; this may be due to imperfect machining of the notch at the initial end or to a serious loss of fixity at the final end where the specimen completely separates. Such values are excluded from the calculation of the average surface work for a single specimen.

APPENDIX E

List of Tables

TABLE I

Fracture Surface Energy of CTBN
Modified EPON 828 Cured* with Curing Agent D**

Type CTBN	CTBN Conc. (pph)	Fracture Surface Energy (10^5 ergs/cm^2)
R 151 W (10%)	10.0	13.0
R 151 W (8%) + 20-64 (2%)	10.0	16.6
R 151 W (6%) + 20-64 (4%)	10.0	15.4
R 151 W (4%) + 20-64 (6%)	10.0	15.1
R 151 W (2%) + 20-64 (8%)	10.0	14.1
20-64 (10%)	10.0	6.9
EPON 828 (unmodified)	--	1.92

*Cured at 120°C for two hours. Post cured at 130°C for two hours.

**5 pph Curing Agent D

TABLE II

Ultimate Tensile Strength of CTBN Modified EPON 828 Cured* with Curing Agent D**

Type CTBN	CTBN Conc. (pph)	Ultimate Tensile Strength (psi)
R 151 W (10%)	10.0	8,020
R 151 W (8%) + 20-64 (2%)	10.0	9,150
R 151 W (6%) + 20-64 (4%)	10.0	9,100
R 151 W (4%) + 20-64 (6%)	10.0	8,975
R 151 W (2%) + 20-64 (8%)	10.0	8,800
20-64	10.0	9,660
EPON 828 (Unmodified)	-	10,170

*Cured at 120°C for two hours. Post cured at 130°C for two hours.

**5 pph Curing Agent D

TABLE III

Uniaxial Compressive Strength of CTBN Modified EPON 828 Cured* with Curing Agent D**

Type CTBN	CTBN Conc. (pph)	Uniaxial Compressive Strength (psi)
R 151 W	10.0	9,700
20-64	10.0	11,300
EPON 828 (Unmodified)	-	12,600

*Cured at 120°C for two hours, Post cured at 130°C for two hours.

**5 pph Curing Agent D.

TABLE IV

Biaxial Tensile Specimen Yield Stress
of CTBN R-151W Modified EPON 828

Specimen Number	Tensile Stress (Ksi)	Hoop Stress (Ksi)
10	8.70	0.00
11	0.00	8.16
12	6.85	8.10
13	7.16	8.59
14	7.09	8.45
15	7.15	7.97
16	7.94	5.90
17	8.75	3.00
18	4.45	9.40
19	2.80	9.50
37	5.26	8.56
38	2.14	8.98

TABLE V

Biaxial Compressive Specimen Yield Stress
of CTBN R-151W Modified EPON 828

Specimen Number	Compressive Stress (ksi)	Hoop Stress (ksi)
36	9.60	0.00
39	0.92	7.60
40	1.73	7.00
41	5.00	5.15
42	6.75	3.54
43	4.50	5.56
44	8.90	1.55
45	0.00	8.60

TABLE VI

Biaxial Compressive Specimen Yield Stress
of CTBN 20-64 Modified EPON 828

Specimen Number	Compressive Stress (ksi)	Hoop Stress (ksi)
20	10.10	0.00
21	0.00	9.71
22	5.80	4.80
23	1.99	8.00
24	5.00	6.15
25	7.95	3.00
26	3.12	7.32
27	9.16	1.50

TABLE VII

Biaxial Compressive Specimen Yield Stress of Unmodified EPON 828

Specimen Number	Compressive Stress (ksi)	Hoop Stress (ksi)
28	12.05	0.00
29	0.00	10.50
30	1.16	9.45
31	3.71	7.94
32	5.90	6.50
33	9.58	1.86
34	8.50	4.01
35	10.7	2.00

APPENDIX F

List of Figures

List of Figures (Cont.)

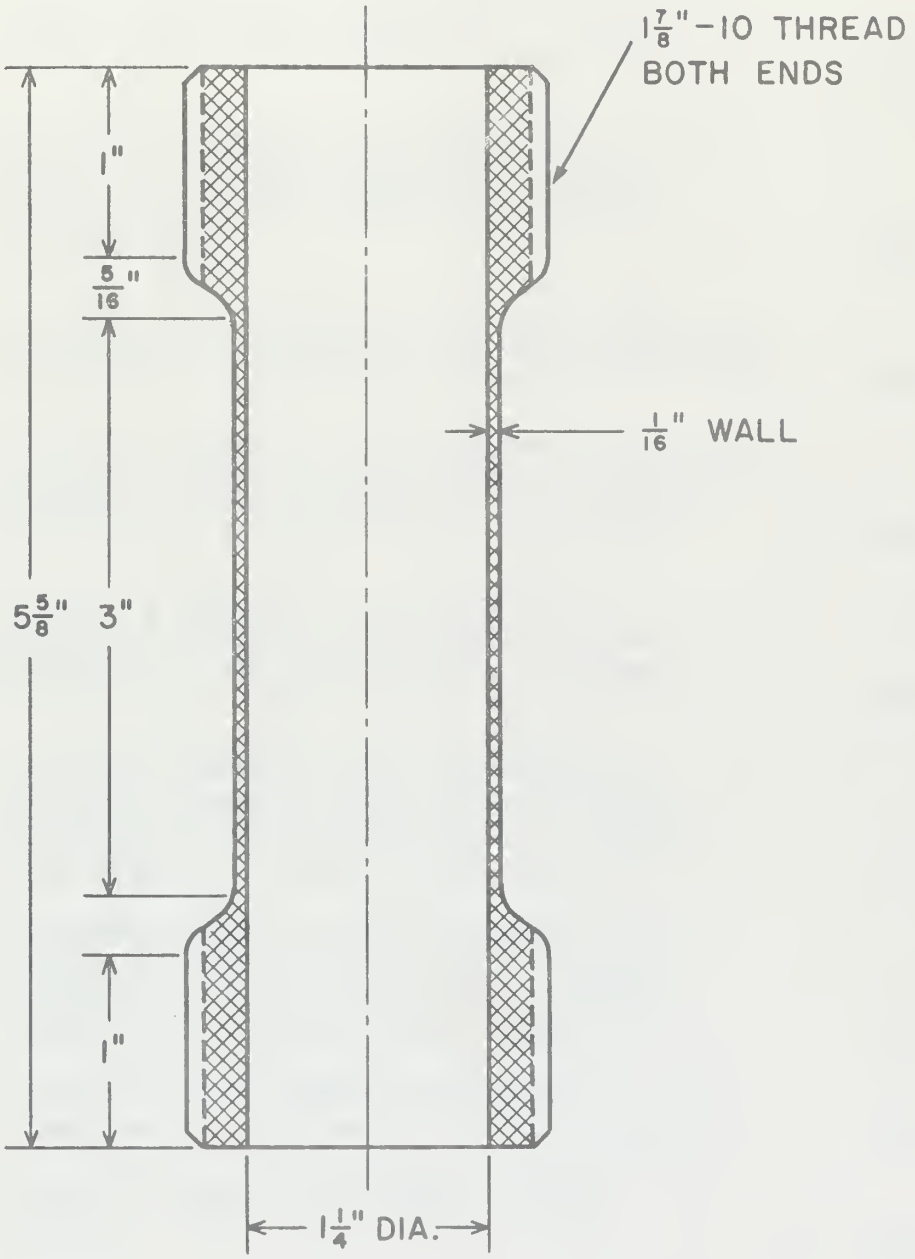

FIGURE 5. BIAXIAL TENSILE SPECIMEN.

List of Figures (Cont.)

List of Figures (Cont.)

FIGURE 1. BIAXIAL TESTING APPARATUS, SHOWN LEFT TO RIGHT, INSTRON CABINET, NITROGEN CYLINDER WITH REGULATOR VALVE, HYDRAULIC ACCUMULATOR FLASK WITH VALVES AND HYDRAULIC PRESSURE GAUGE, AND INSTRON GRIPS WITH BIAXIAL COMPRESSIVE SPECIMEN BETWEEN THE CROSSHEAD AND LOAD CELL.

FIGURE 2. BIAXIAL SPECIMEN MACHINING PROCESS. SHOWN LEFT TO RIGHT, HOLLOW CYLINDRICAL CASTING, MACHINED BIAXIAL TENSILE SPECIMEN, AND MACHINED BIAXIAL COMPRESSIVE SPECIMEN.

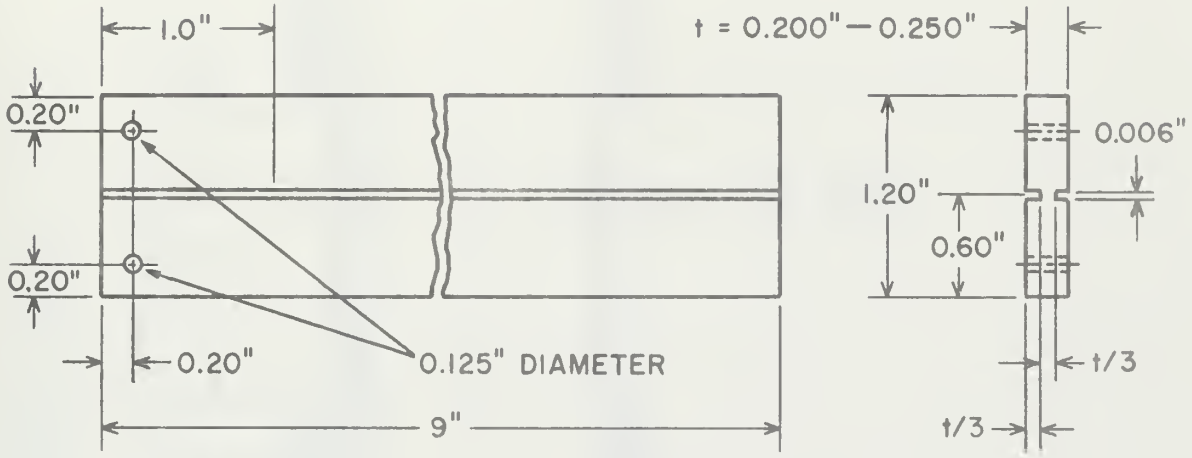

FIGURE 3. CLEAVAGE SPECIMEN.

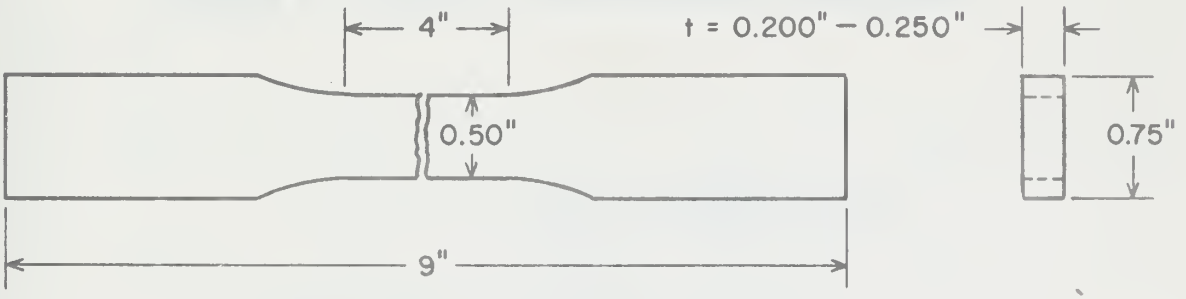

FIGURE 4. UNIAXIAL TENSILE SPECIMEN.

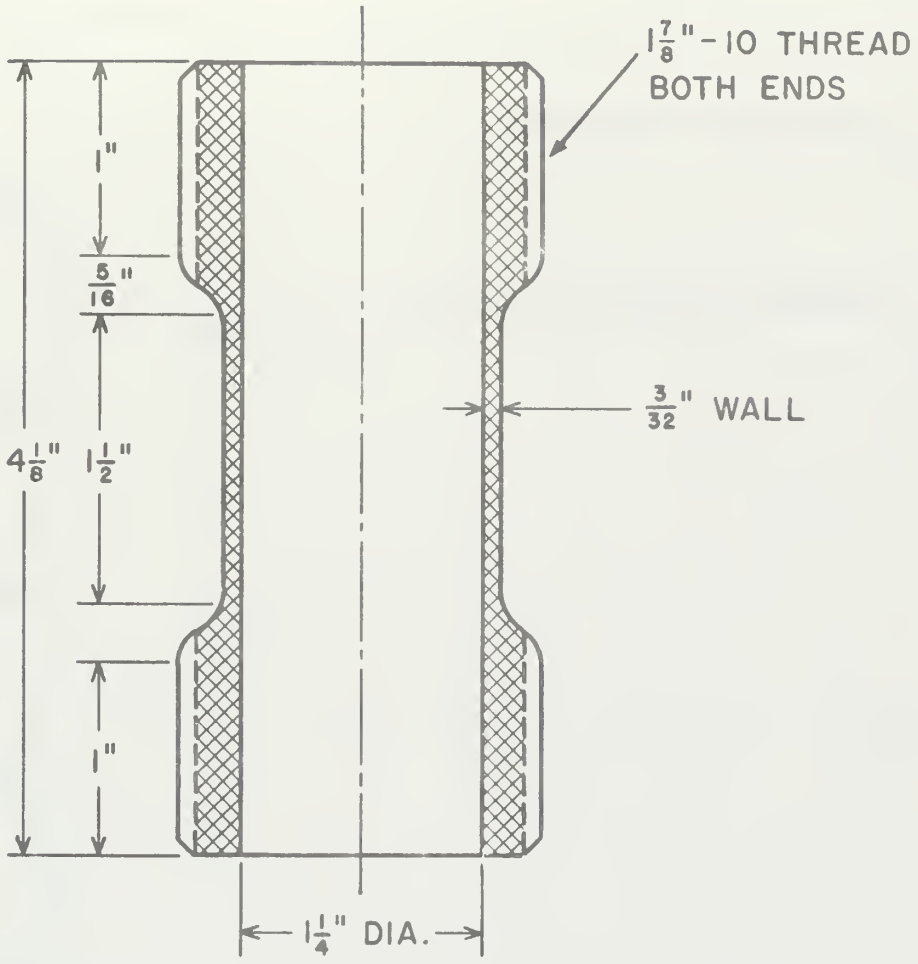

FIGURE 6. BIAXIAL COMPRESSIVE SPECIMEN.

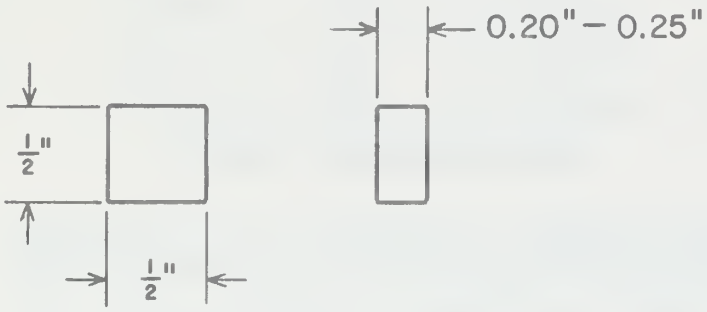

FIGURE 7. UNIAXIAL COMPRESSIVE SPECIMEN.

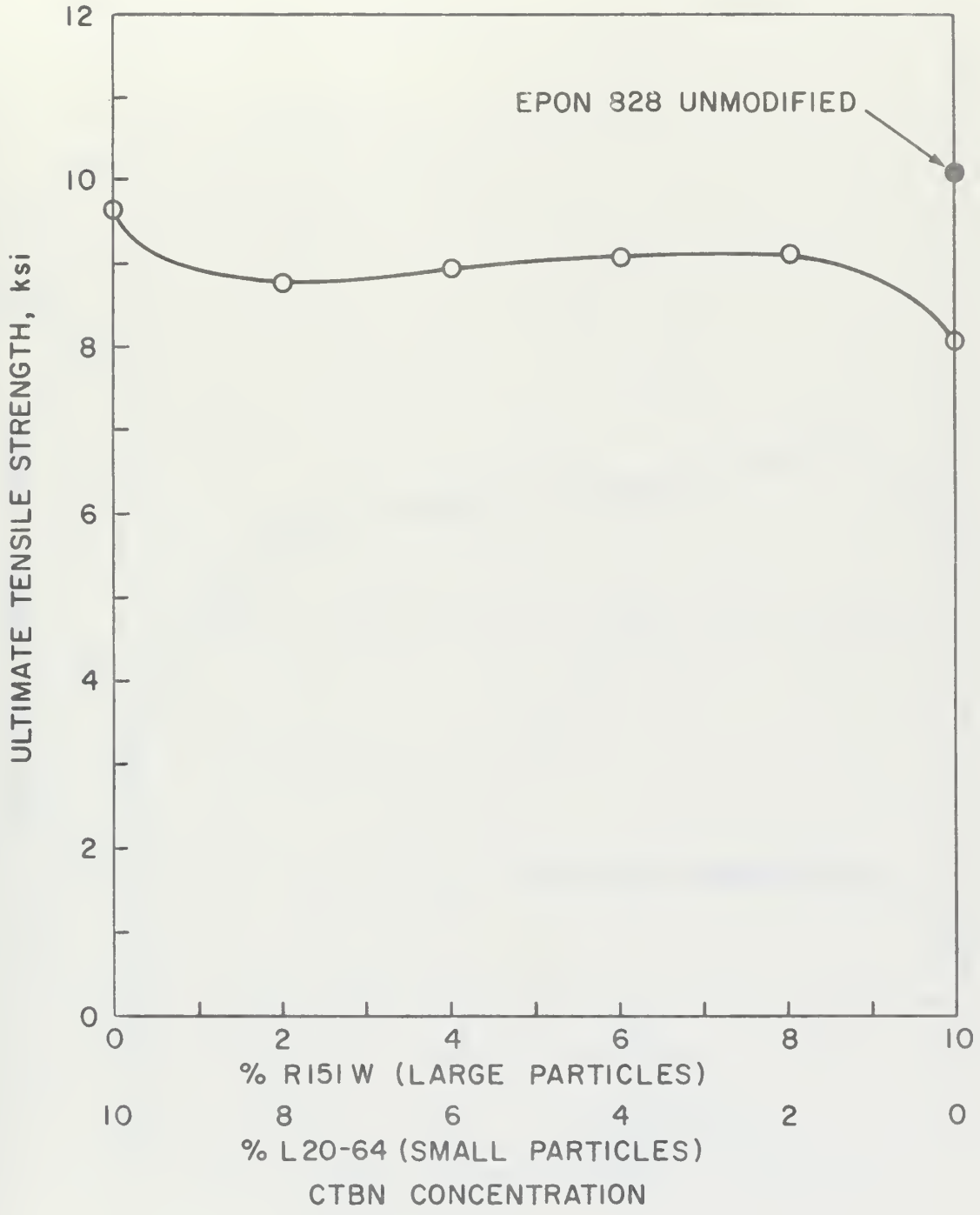

FIGURE 8. VARIATION OF ULTIMATE TENSILE STRENGTH WITH CTBN CONCENTRATION 10 pph BY WEIGHT THROUGHOUT FOR RUBBER MODIFIED EPON 828, CURED WITH 5 pph CURING AGENT D.

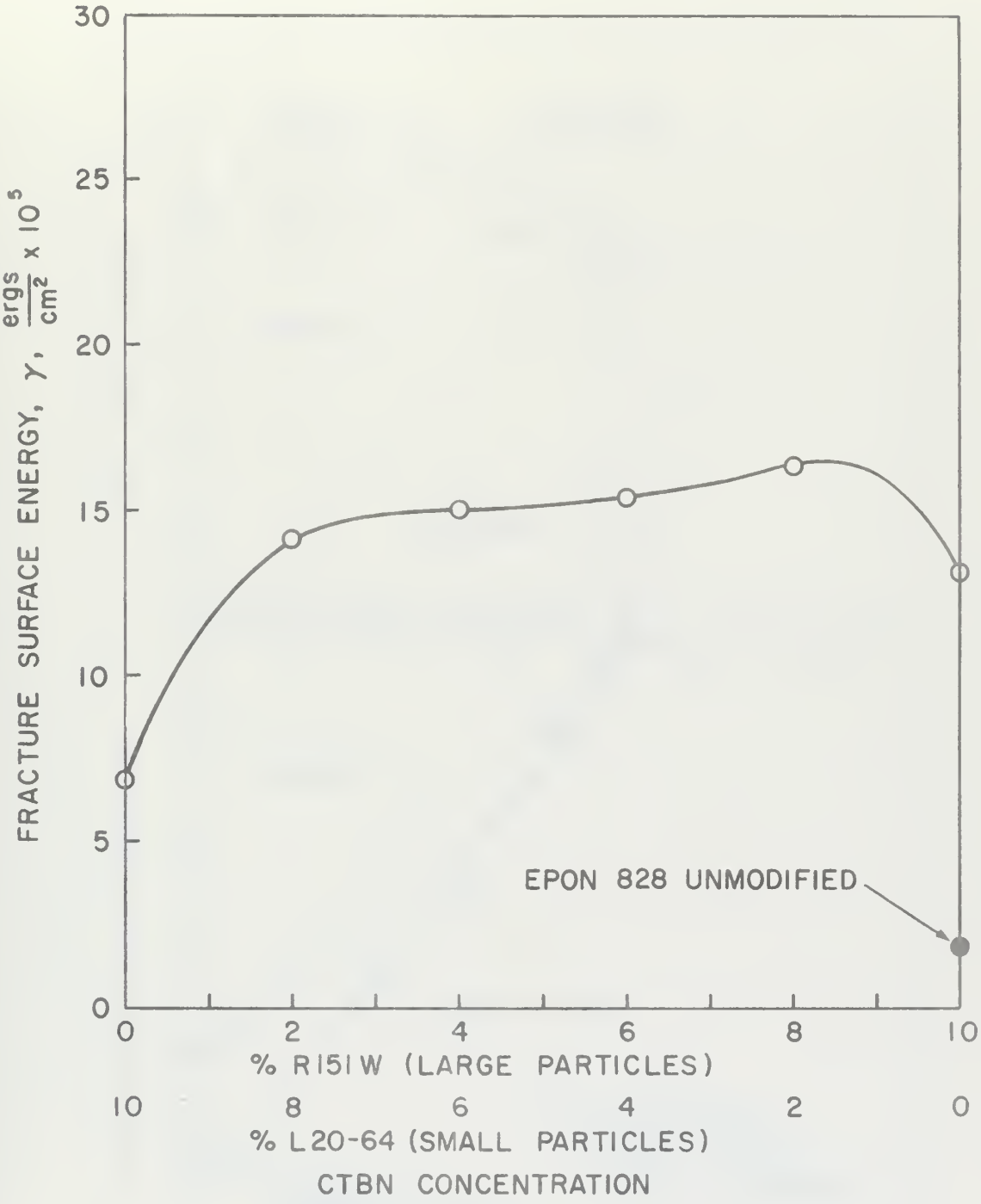

FIGURE 9. VARIATION OF FRACTURE SURFACE ENERGY WITH CTBN CONCENTRATION 10 pph BY WEIGHT THROUGHOUT FOR RUBBER MODIFIED EPON 828, CURED WITH 5 pph CURING AGENT D.

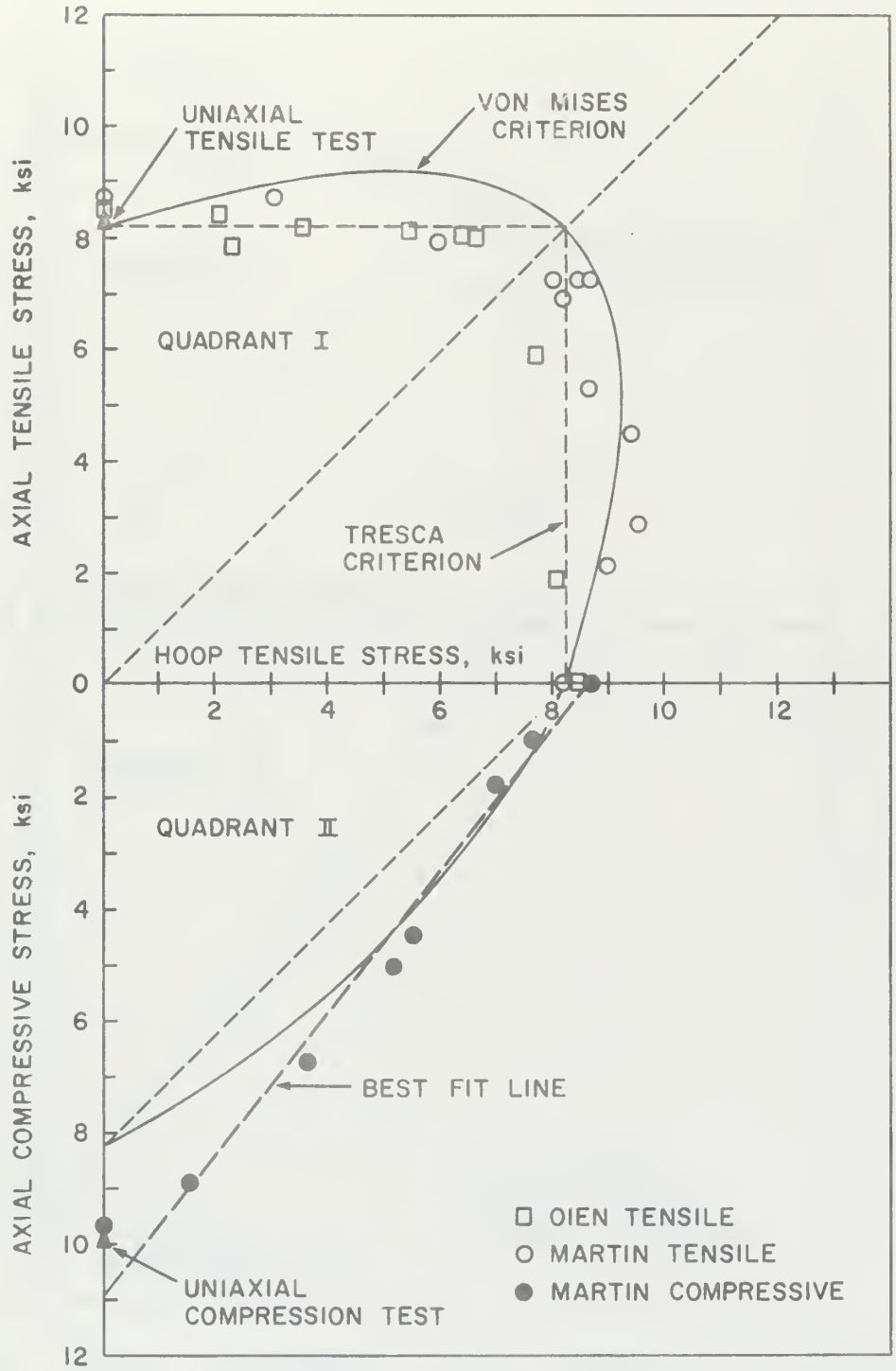

FIGURE 10. BIAXIAL SPECIMEN. AXIAL TENSILE/COMPRESSIVE STRESS, σ_T / σ_c, vs. HOOP TENSILE STRESS, σ_h, FOR EPON 828 MODIFIED WITH 10% BY WEIGHT OF CTBN 151W (LARGE PARTICLES).

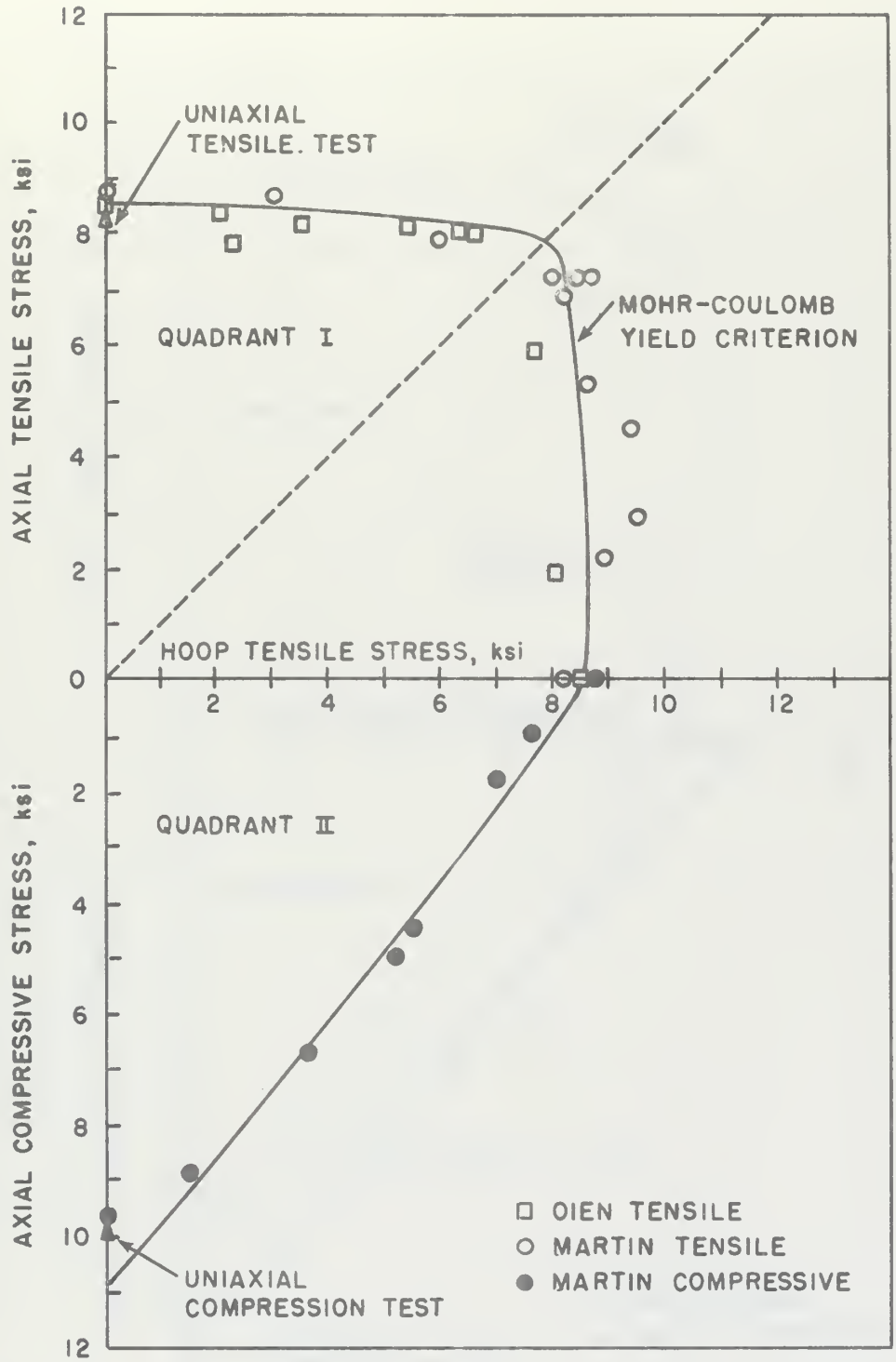

FIGURE 10a. BIAXIAL SPECIMEN. AXIAL TENSILE/COMPRESSIVE STRESS, σ_t / σ_c, vs. HOOP TENSILE STRESS, σ_h, FOR EPON 828 MODIFIED WITH 10% BY WEIGHT OF CTBN 151W (LARGE PARTICLES).

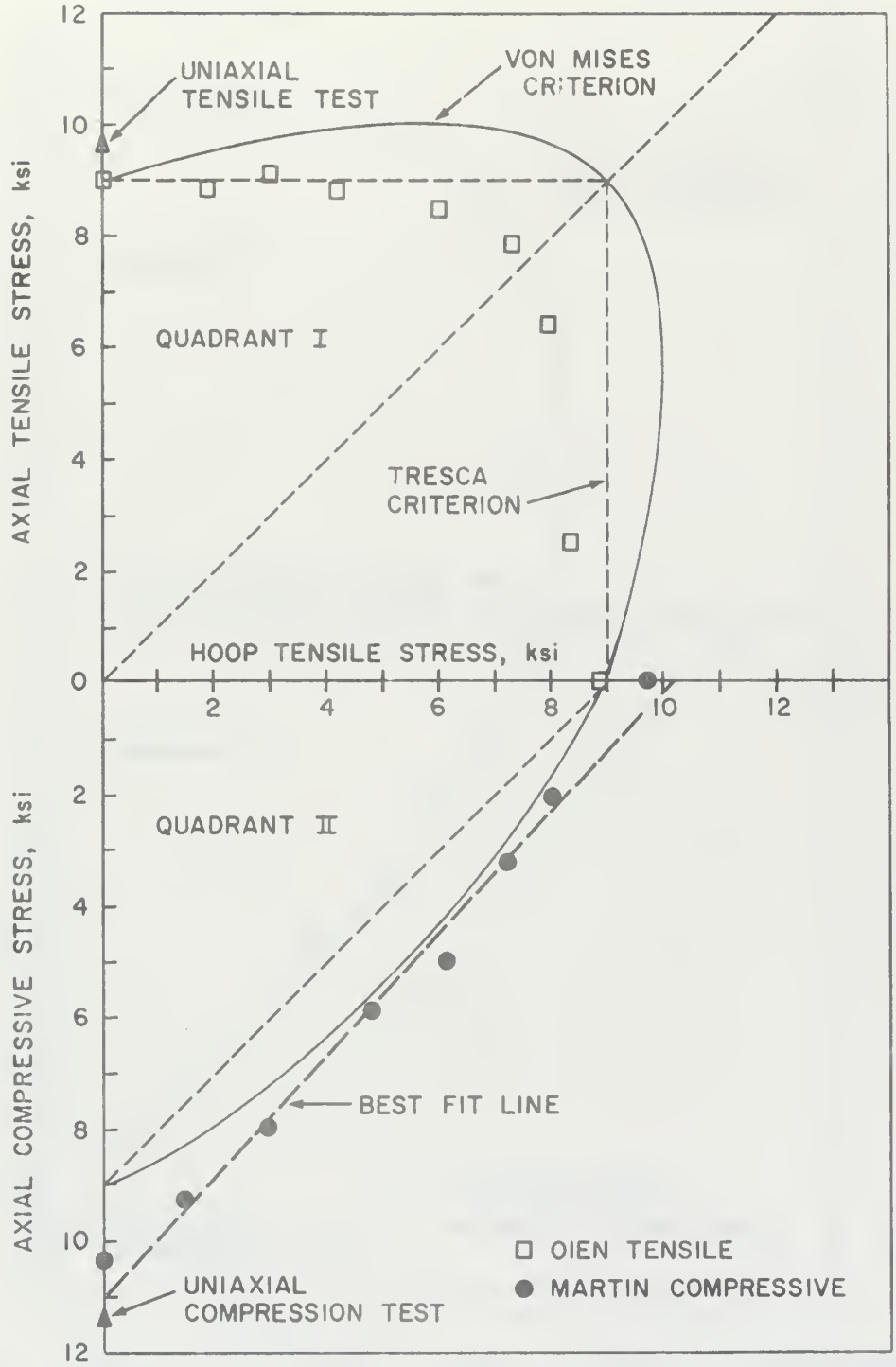

FIGURE 11. BIAXIAL SPECIMEN. AXIAL TENSILE/COMPRESSIVE STRESS, σ_T / σ_c, vs. HOOP TENSILE STRESS, σ_h, FOR EPON 828 MODIFIED WITH 10% BY WEIGHT OF CTBN 20-64 (SMALL PARTICLES).

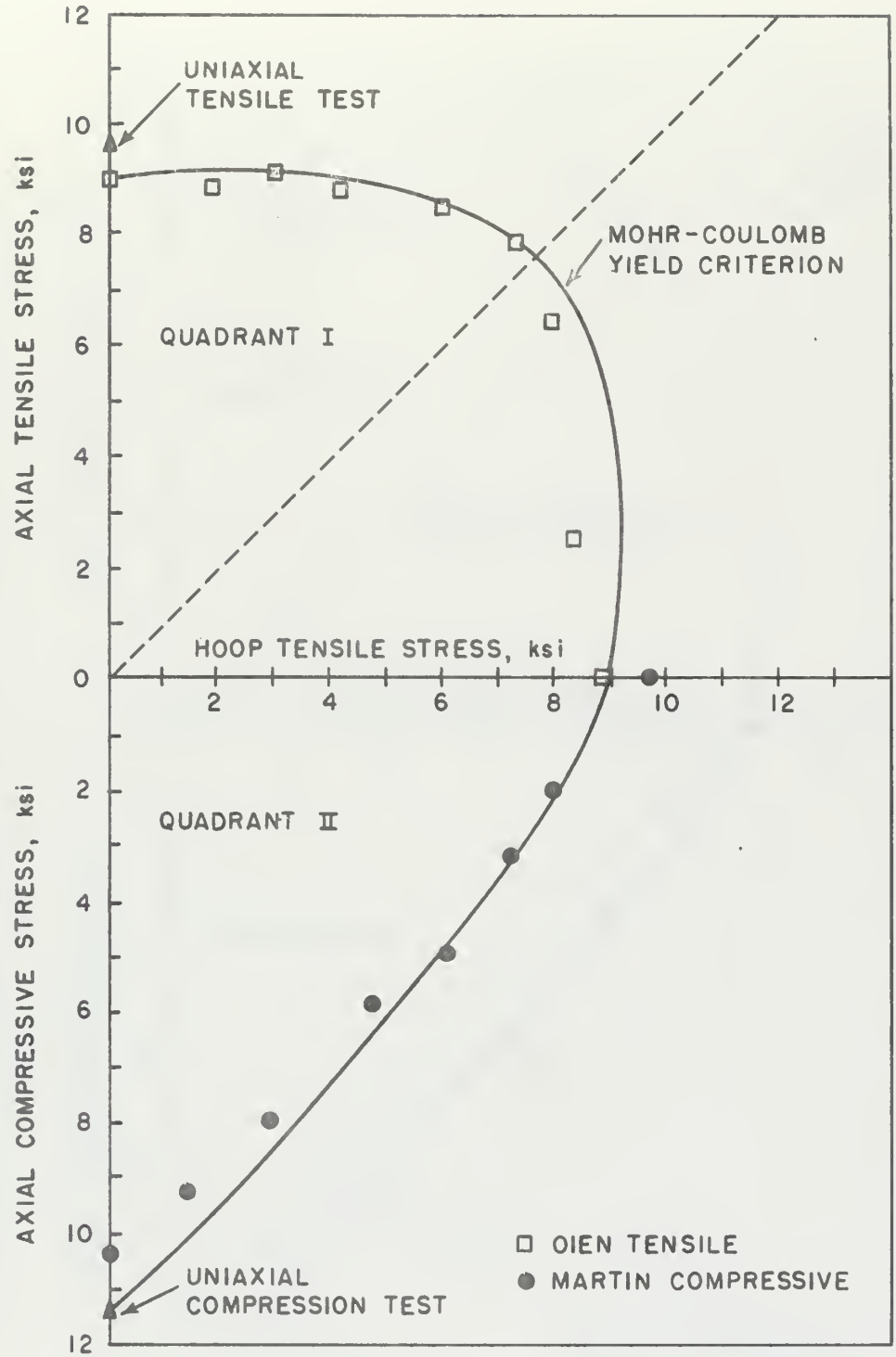

FIGURE 11a. BIAXIAL SPECIMEN. AXIAL TENSILE/COMPRESSIVE STRESS, σ_T / σ_C, vs. HOOP TENSILE STRESS, σ_h, FOR EPON 828 MODIFIED WITH 10% BY WEIGHT OF CTBN 20-64 (SMALL PARTICLES).

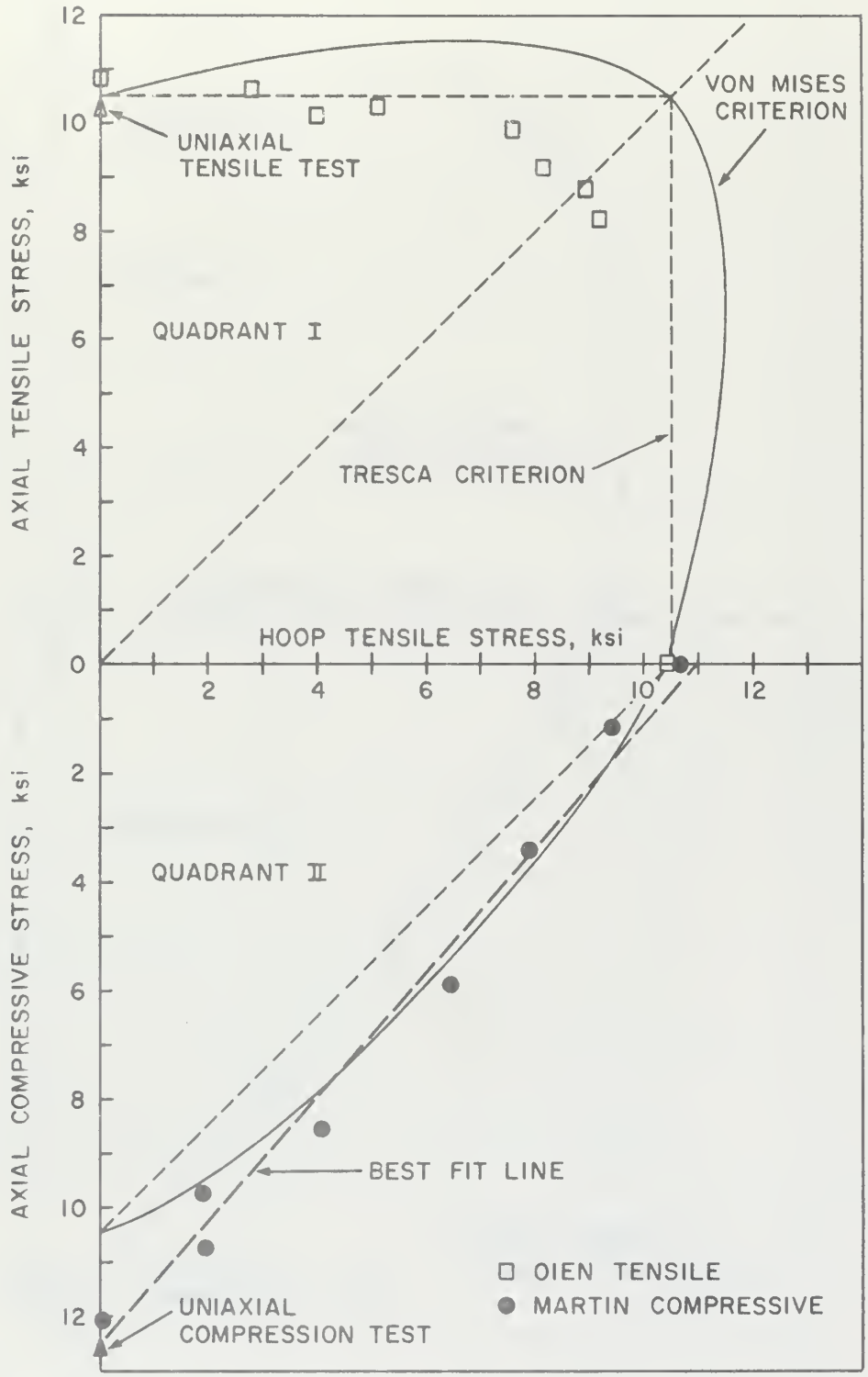

FIGURE 12. BIAXIAL SPECIMEN. AXIAL TENSILE/COMPRESSIVE STRESS, σ_T/σ_c, vs. HOOP TENSILE STRESS, σ_h, FOR EPON 828 UNMODIFIED.

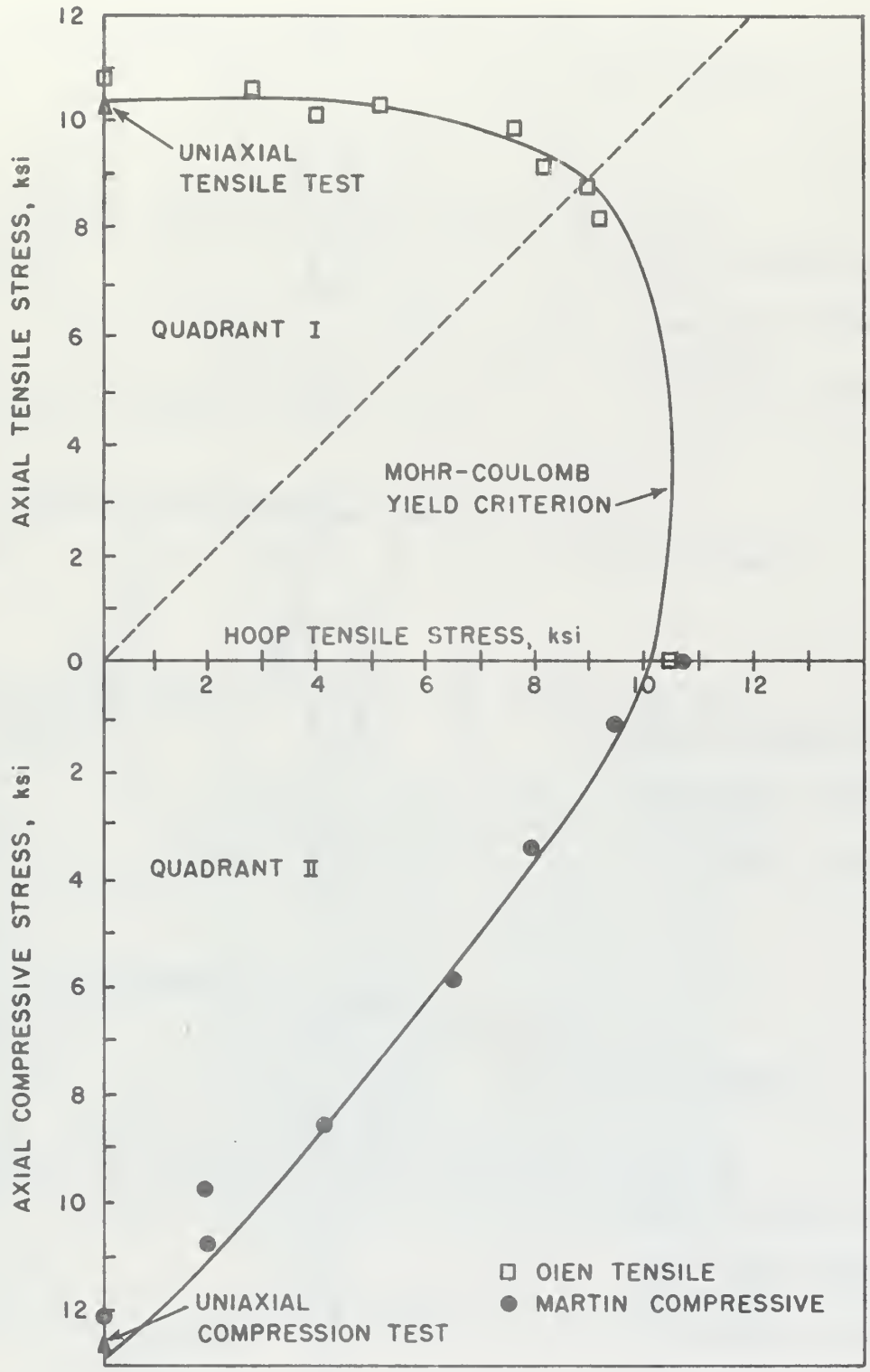

FIGURE 12a. BIAXIAL SPECIMEN. AXIAL TENSILE/COMPRESSIVE STRESS, σ_T / σ_C, vs. HOOP TENSILE STRESS, σ_h, FOR EPON 828 UNMODIFIED.

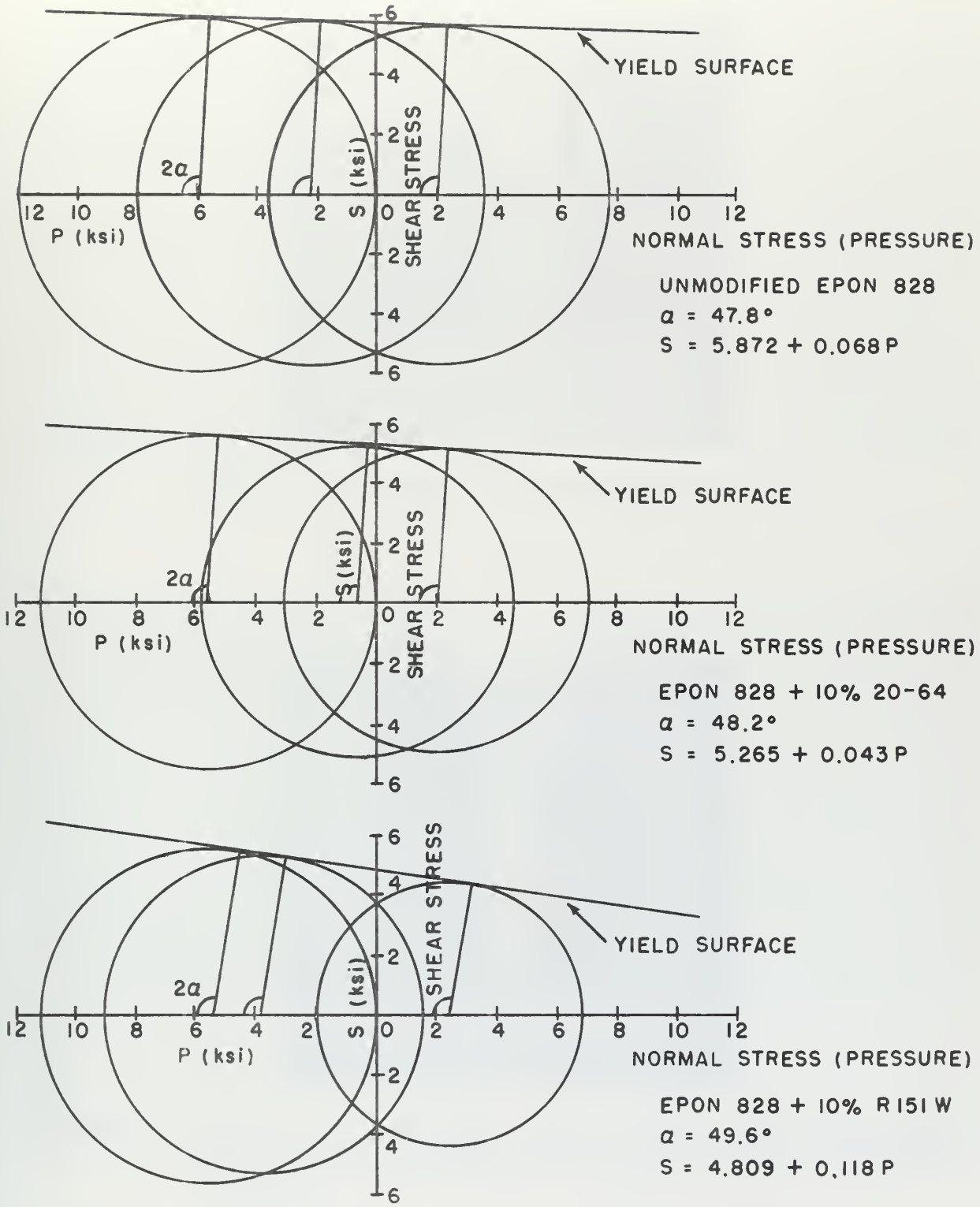

FIGURE 12b. MOHR'S CIRCLE DIAGRAMS CONSTRUCTED FROM THE DATA IN THE SECOND QUADRANT OF FIGURES 10-12.

FIGURE 13. FRACTURED BIAXIAL SPECIMEN CASTINGS.

FIGURE 14. FAILED BIAXIAL SPECIMEN. SHOWN LEFT TO RIGHT, FRACTURED BIAXIAL TENSILE SPECIMEN AND YIELDED BIAXIAL COMPRESSIVE SPECIMEN.

EPON 828 + 5 pph CURING AGENT D
(330X)

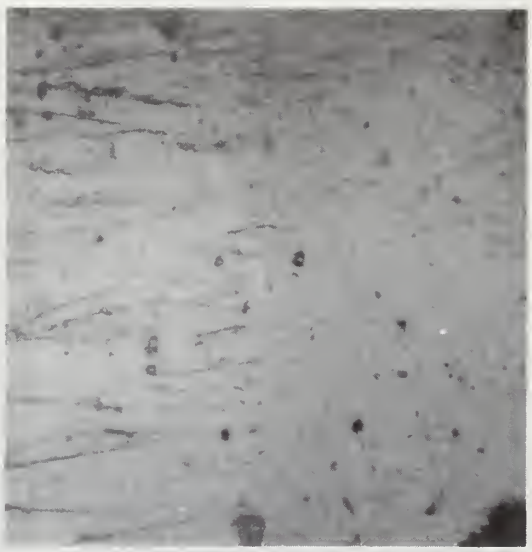

EPON 828 + 10 pph 20-64 +
5 pph CURING AGENT D (562.5X)

EPON 828 + 10 pph R-151 +
5 pph CURING AGENT D (137.5X)

EPON 828 + 2 pph R-151 + 8 pph
20-64 + 5 pph CURING AGENT D (137.5X)

FIGURE 15. OPTICAL MICROGRAPH OF CLEAVAGE SURFACES IN THE REGION OF TRANSITION BETWEEN FAST (RIGHT) AND SLOW (LEFT) CRACK PROPAGATION.

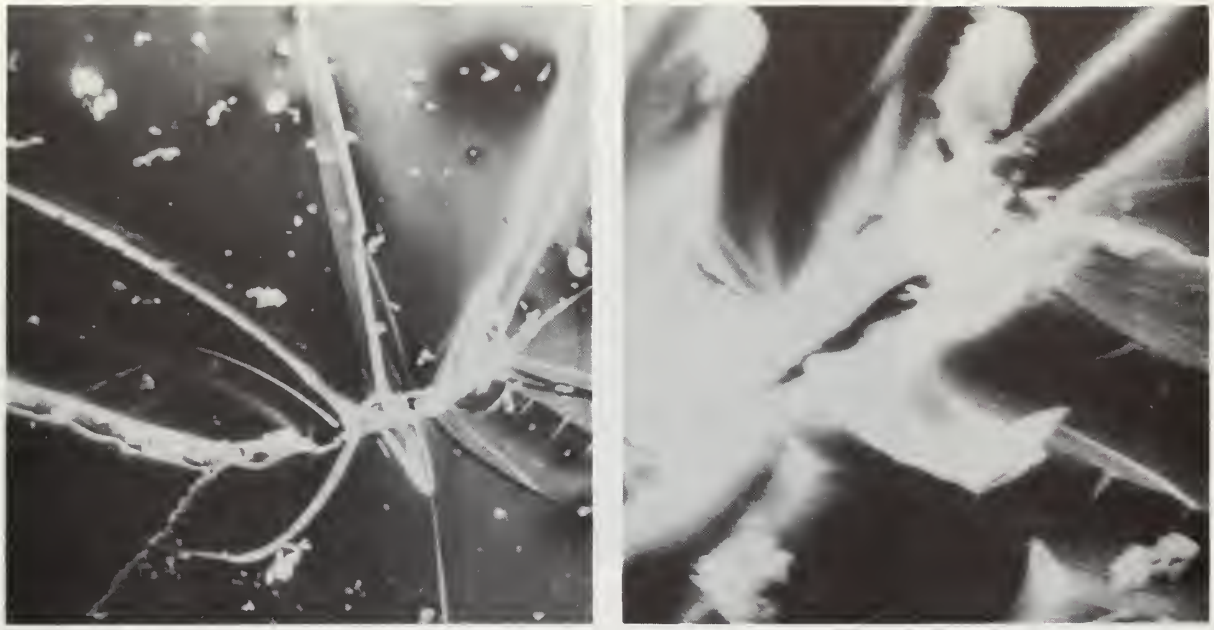

(320X) (1300X)

FIGURE 16. SCANNING ELECTRON MICROGRAPH OF THE FRACTURE SURFACE AT A FLAW OF A TENSILE SPECIMEN; EPON 828 + 10 pph CTBN 20-64 (SMALL PARTICLES) + 5 pph CURING AGENT D.

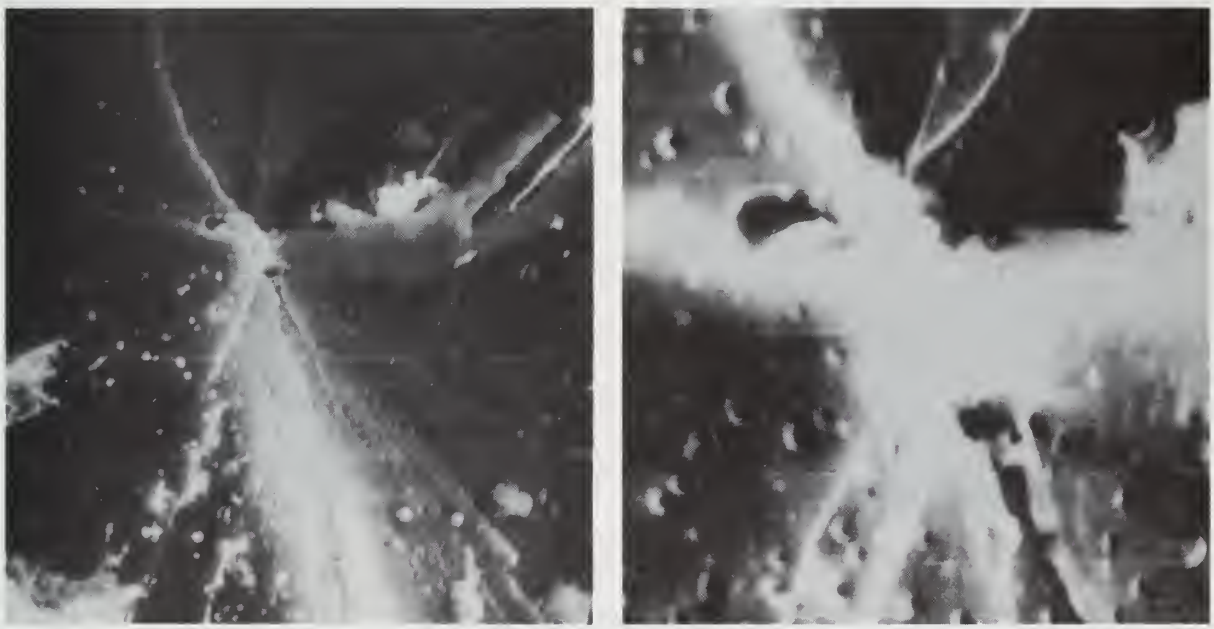

(320X) (1800X)

FIGURE 17. SCANNING ELECTRON MICROGRAPH OF THE FRACTURE SURFACE AT A FLAW OF A TENSILE SPECIMEN; EPON 828 + 2 pph CTBN R-151 (LARGE PARTICLES) + 8 pph CTBN 20-64 (SMALL PARTICLES) + 5 pph CURING AGENT D.

FIGURE 18. OPTICAL MICROGRAPH OF THE FRACTURE SURFACE AT A FLAW OF A TENSILE SPECIMEN; EPON 828 + 5 pph CURING AGENT D. (55X).

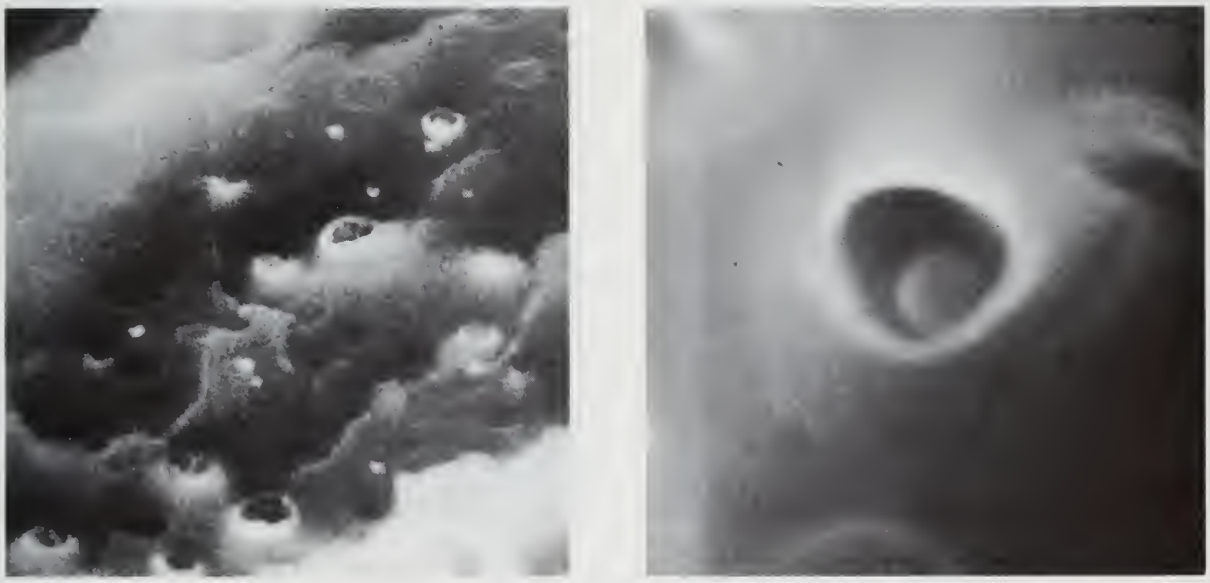

(2400X) (16,000X)

FIGURE 19. SCANNING ELECTRON MICROGRAPH OF THE FRACTURE SURFACE OF A TENSILE SPECIMEN; EPON 828 + 10 pph CTBN R-151 (LARGE PARTICLES) + 5 pph CURING AGENT D.

TRANSITION ZONE (320X)

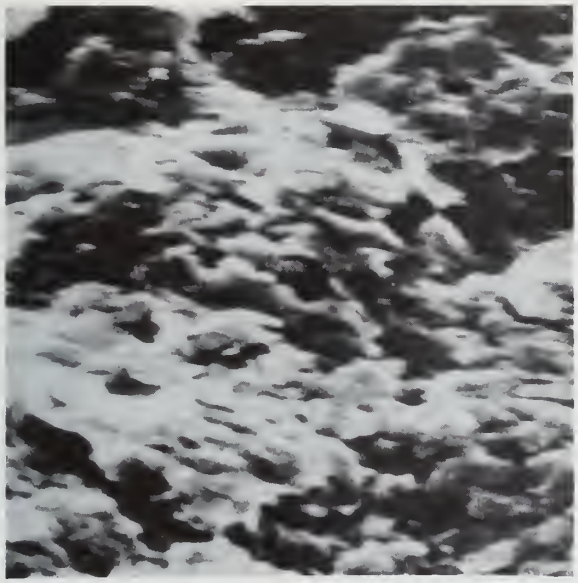

FAST CRACK PROPAGATION (5000X)

SLOW CRACK PROPAGATION (1200X)

FIGURE 20. SCANNING ELECTRON MICROGRAPHS OF CLEAVAGE SPECIMEN FRACTURE SURFACE; EPON 828 + 10 pph CTBN 20-64 (SMALL PARTICLES) + 5 pph CURING AGENT D.

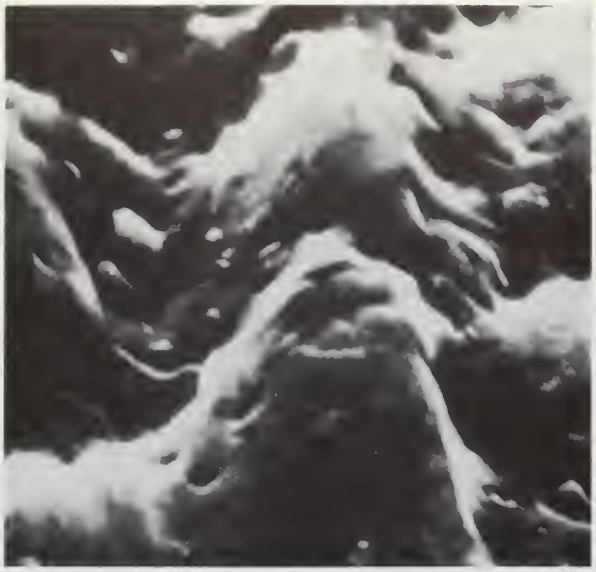

FAST CRACK PROPAGATION
(5000X)

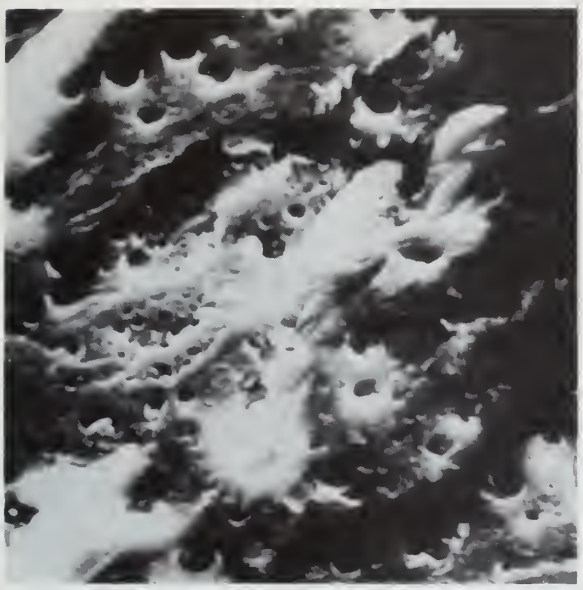

SLOW CRACK PROPAGATION
(1400X)

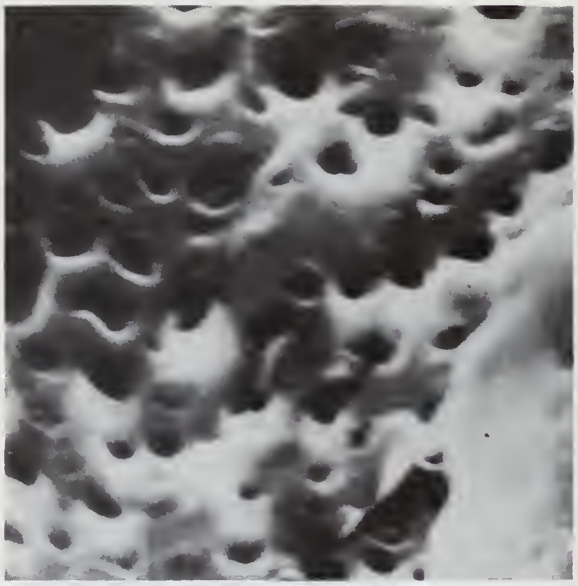

SLOW CRACK PROPAGATION
(5000X)

FIGURE 21. SCANNING ELECTRON MICROGRAPHS OF CLEAVAGE SPECIMEN FRACTURE SURFACE; EPON 828 + 10 pph CTBN R-151 (LARGE PARTICLES) + 5 pph CURING AGENT D.

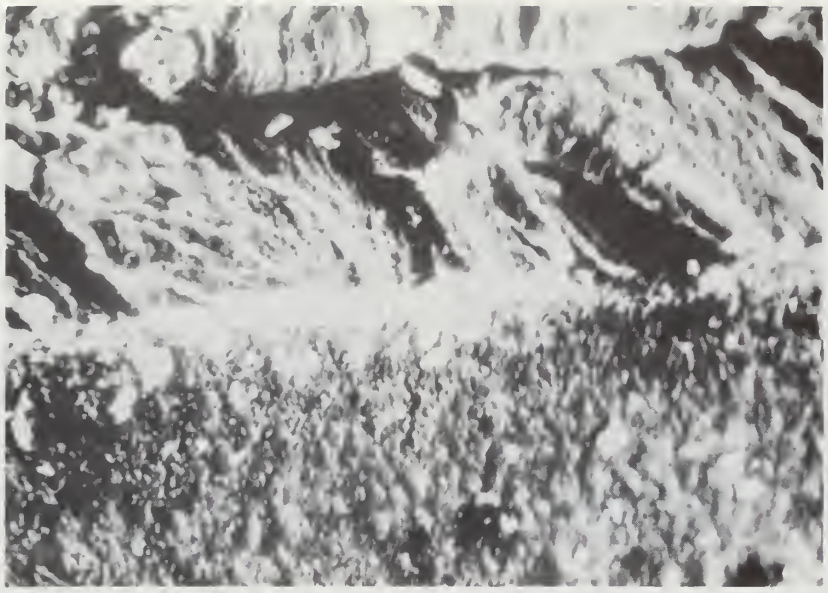

TRANSITION ZONE (340X)
TOP: SLOW CRACK PROPAGATION
BOTTOM: FAST CRACK PROPAGATION

FAST CRACK PROPAGATION
(2000X)

SLOW CRACK PROPAGATION
(3400X)

FIGURE 22. SCANNING ELECTRON MICROGRAPHS OF CLEAVAGE SPECIMEN FRACTURE SURFACE; EPON 828 + 2 pph CTBN R-151 (LARGE PARTICLES) + 8 pph CTBN 20-64 (SMALL PARTICLES) + 5 pph CURING AGENT D.

UNMODIFIED EPON 828

EPON 828 + 10 pph CTBN 20-64
(SMALL PARTICLES)

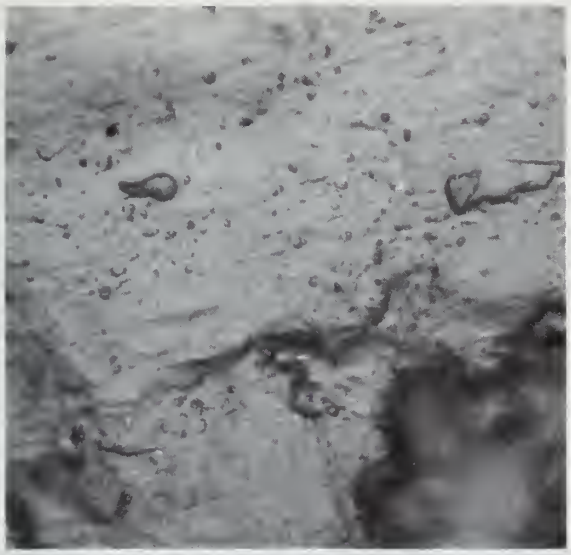

EPON 828 + 10 pph CTBN R-151
(LARGE PARTICLES)

EPON 828 + 10 pph CTBN 107-468-171A
(VERY LARGE PARTICLES)

FIGURE 23. OPTICAL MICROGRAPHS OF BIAXIAL COMPRESSIVE SPECIMEN YIELD SURFACES. (450X).

FIGURE 24. BIAXIAL TENSILE SPECIMEN YIELD SURFACE; EPON 828 + 10 pph CTBN R-151 (LARGE PARTICLES). (450X).

FIGURE 25.
BIAXIAL COMPRESSIVE SPECIMEN FRACTURE SURFACE; EPON 828 + 10 pph CTBN R-151 (LARGE PARTICLES). (450X).

FIGURE 26.
BIAXIAL COMPRESSIVE SPECIMEN FRACTURE SURFACE AT CRACK EDGE, CTBN R-151 (LARGE PARTICLES). (450X).

10 pph CTBN 20-64
(28% Acrylonitrile)

10 pph CTBN R-151
(18% Acrylonitrile)

2 pph CTBN 20-64
8 pph CTBN R-151

FIGURE 27. PARTICLE SIZE AND MORPHOLOGY FOR RUBBER MODIFIED, CURING AGENT D (5 pph) CURED EPON 828. PLATE CASTINGS. CURING TEMPERATURE 120°C. (28,600X).

10 pph CTBN R-151 (18% Acrylonitrile)

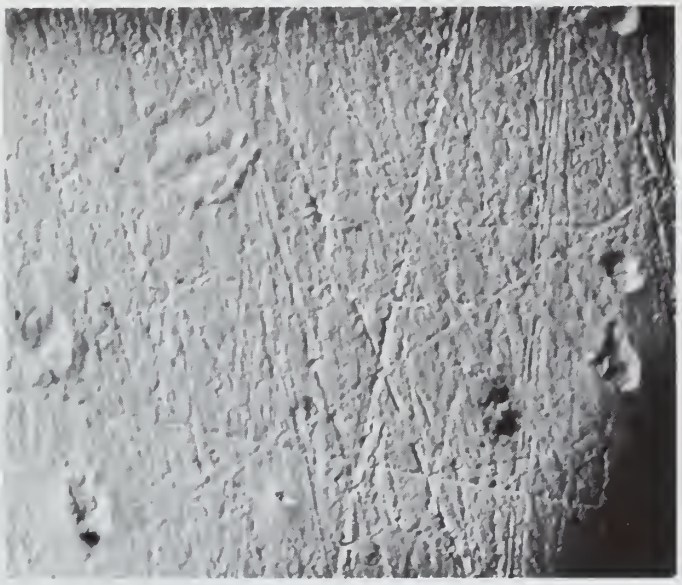

2 pph CTBN 20-64 (28% Acrylonitrile)
8 pph CTBN R-151 (18% Acrylonitrile)

FIGURE 28. PARTICLE SIZE AND MORPHOLOGY FOR RUBBER MODIFIED, CURING AGENT D (5 pph) CURED EPON 828. PLATE CASTINGS. CURING TEMPERATURE 120°C. (9550X).

Thesis
M3575 Martin
Effects of variation of the modifying CTBN elastomer in thermoset polymers.
127306